

# Theoretical isochrones from models with new radiative opacities\*

G. Bertelli<sup>1,3</sup>, A. Bressan<sup>2</sup>, C. Chiosi<sup>3</sup>, F. Fagotto<sup>3</sup> and E. Nasi<sup>2</sup>

<sup>1</sup> National Council of Research (CNR-GNA)

<sup>2</sup> Astronomical Observatory, Vicolo dell'Osservatorio 5, I-35122 Padova, Italy

<sup>3</sup> Department of Astronomy, Padova University, Vicolo dell'Osservatorio 5, I-35122 Padova, Italy

Received January 25; accepted March 11, 1994

**Abstract.** — In this paper we present large grids of theoretical isochrones for the initial chemical compositions  $[Z=0.0004, Y=0.23]$ ,  $[Z=0.004, Y=0.24]$ ,  $[Z=0.008, Y=0.25]$ ,  $[Z=0.02, Y=0.28]$ , and  $[Z=0.05, Y=0.352]$  and ages in the range  $4 \cdot 10^6$  yr to  $16 \cdot 10^9$  yr. These isochrones are derived from stellar models computed with the most recent radiative opacities by Iglesias et al. (1992). In addition to this we present another set with chemical composition  $[Z=0.001, Y=0.23]$  based on models calculated with the radiative opacities by Huebner et al. (1977). All the stellar models are followed from the zero age main sequence (ZAMS) to the central carbon ignition for massive stars or to the beginning of the thermally pulsing regime of the asymptotic giant branch phase (TP-AGB) for low and intermediate mass stars. For each isochrone, we give the current mass, effective temperatures, bolometric and visual magnitudes,  $(U - B)$ ,  $(B - V)$ ,  $(V - R)$ ,  $(V - I)$ ,  $(V - J)$ ,  $(V - H)$ , and  $(V - K)$  colors, and the luminosity function for the case of the Salpeter law. In addition to this, integrated magnitudes and colors at several characteristic points are also presented together with the mass of the remnant star when appropriate. The main characteristic that makes this set of isochrones very valuable is based on their extension in mass and chemical composition, besides the calculation of late stages of evolution, beyond the red giant tip till the white dwarf stage after the planetary nebula phase.

**Key words:** stars: evolution, interiors, fundamental parameters, HR diagram

## 1. Introduction

The computations of new radiative opacities (OPAL) by Rogers & Iglesias (1992) and Iglesias et al. (1992) gave the start to a great deal of work aiming to evaluate if the opacity changes were or not sufficient to remove all discrepancies between stellar evolution theory and observations of star clusters, associations, variable stars, etc. (Stothers & Chin 1991; Moskalik et al. 1992; Langer 1992; Chiosi et al. 1992). There is general agreement that the effects due to the adoption of OPAL instead of the Los Alamos (LAOL) by Huebner et al. (1977) opacities are significant, even if not so large as for the comparison between OPAL and the old Cox & Stewart (1970a,b) ones. It must also be remarked that there are differences also among the various tables of radiative opacities published over the last few years by the Livermore group, and that in our computations the most recent ones by Iglesias et al. (1992) are adopted, including the spin-orbit interaction in the treatment of Fe atomic data, and adopting the recent measurement of the solar photospheric Fe abundance by Grevesse (1991) and Hannaford et al. (1992).

The great deal of recent accurate data for the stellar content of rich, young and intermediate age clusters in the Magellanic Clouds as well as of globular and old open clusters in the Milky Way, offer unparalleled opportunities for the study of stellar evolution, bringing into evidence that there are many problems still unsolved when comparing theory and observations. Among others, we recall the problems raised by the observed distribution of massive stars in the HR diagram (HRD), the evolutionary status of SN 1987A progenitor, the study of the C-M diagrams (CMD) and luminosity functions (LF) of intermediate age clusters in the Large Magellanic Cloud, of the Galactic old open clusters, and finally the determination of the basic parameters of globular clusters. All these topics have been amply discussed in literature, cf. the recent review by Chiosi et al. (1992) and references therein.

In order to improve upon the agreement of stellar models with observations, a continuous updating of the existing evolutionary codes is operated to produce new grids of models. Among others, Schaller et al. (1992), Schaerer et al. (1993a,b), Alongi et al. (1993), Bressan et al. (1993a), and Fagotto et al. (1994a,b) computed the most recent and updated evolutionary sets for different chemical compositions.

\*Tables 1 to 6 are only available in electronic form: see the Editorial in A&AS 1994, Vol. 103, No. 1

In this paper, we present isochrones derived from evolutionary sequences for various choices of the initial chemical composition and with mass loss by stellar wind for massive stars. Each evolutionary track has been followed from the main sequence up to the final stage, namely the tip of the RGB, or the start of the TP-AGB, or finally the stage of carbon-ignition in a mildly electron degenerate C-O core, depending on the initial mass of the star.

The presentation of the stellar models is limited to a summary of their input physics and main characteristics. For all details the reader should refer to the papers by Alongi et al. (1993), Bressan et al. (1993a), and Fagotto et al. (1994a,b) that amply describe the stellar models in use. On the contrary, we give extensive tabulations of isochrones, integrated magnitudes, colors and luminosity functions.

The isochrones, spanning a wide range of ages, are given in the observational plane of the  $U$ ,  $B$ ,  $V$  pass-bands according to Buser & Kurucz (1978), the  $R$ ,  $I$  Cousins pass-bands as in Bessell (1990), and the  $J$ ,  $H$ ,  $K$  pass-bands as in Bessell & Brett (1988).

The plan of the paper is as follows. In Sect. 2, we present the sets of models together with the main input physics. In Sect. 3, we give some key details on how the isochrones are calculated. In Sect. 4, we present the conversions we have adopted to transfer luminosities and effective temperatures into magnitudes and colors. In Sect. 5, we shortly describe the layout of the isochrone grids and the key information (integrated magnitudes and colors, and luminosity functions) contained in each isochrone. These extensive tabulations of data are not printed here but stored in the electronic archive of Astronomy and Astrophysics at the Centre de Données Stellaires (CDS) in Strasbourg, from which they can be retrieved with the standard procedure. For the sake of an easy usage of these isochrones, in Sect. 6 we present summary tables for each chemical composition containing a few characteristic points of each isochrone and various age calibrators. In Sect. 7, we shortly discuss the relation between the initial and final mass of the stars and compare it both with other theoretical results and the empirical relation. Finally, some concluding remarks are drawn in Sect. 8.

## 2. Stellar models

Complete evolutionary sequences have been computed in a series of papers by Bressan et al. (1993a), and Fagotto et al. (1994a,b) for various initial chemical compositions, namely  $[Z=0.0004, Y=0.23]$ ,  $[Z=0.004, Y=0.24]$ ,  $[Z=0.008, Y=0.25]$ ,  $[Z=0.02, Y=0.28]$ , and  $[Z=0.05, Y=0.352]$  adopting the recent radiative opacities by Iglesias et al. (1992). These grids of stellar tracks constitute the starting point of the isochrones described in this paper.

In addition to this, we present also isochrones for the chemical composition  $[Z=0.001, Y=0.23]$  that are derived

from models computed with the opacities by Huebner et al. (1977). These tracks have not yet been published, but as the metal content is low, they would not significantly change if re-computed with the new opacities. The effect of varying the opacity from LAOL to OPAL at low metallicities has been estimated to be small by Alongi et al. (1993). This has been confirmed by the new computations by Fagotto et al. (1993b) for the same chemical composition as in Alongi et al. (1993), namely  $[Z=0.008, Y=0.25]$ . Therefore, even if the set of isochrones with  $Z=0.001$  is not fully homogeneous with the others, it can be safely used for all practical purposes.

The choice of the chemical composition parameters  $Y$  and  $Z$  is made according to the law  $\Delta Y/\Delta Z = 2.5$  that represents a lower limit to the estimates given by Pagel (1989).

For low mass stars ( $M < M_{\text{HeF}}$ , where  $M_{\text{HeF}}$  is the maximum initial mass which develops an electron degenerate core composed of helium), the tracks from the main sequence up to the tip of RGB, and from the beginning of the core He-burning phase up to the start of the thermally pulsing regime of the He-burning shell (TP-AGB) are computed separately. First, this allows us to avoid the complicated evolution from the stage of He-flash down to the horizontal branch (HB), second to easily incorporate the effect of mass loss along the RGB on the location of models on the Zero Age Horizontal Branch (ZAHB) phase (see Renzini 1977).

In the following, we briefly summarize a few relevant points of the input physics of model calculations. A thorough description of properties of these evolutionary sequences can be found in Bressan et al. (1993a) and Fagotto et al. (1994a,b). See also Alongi et al. (1993) for more details.

### 2.1. Overshoot from convective cores and envelopes

The extension of the convective regions, either cores or envelopes, is determined in presence of convective overshoot. The physical motivations for the occurrence of this phenomenon and its efficiency have been discussed recently by Zahn (1991), Canuto & Mazzitelli (1991) and Cattaneo et al. (1991) to whom the reader should refer.

Overshoot from the convective cores is according to Bressan et al. (1981), whereas that from the convective envelopes is as in Alongi et al. (1991). The extension of the overshoot regions is governed by the parameters  $\Lambda_c$  and  $\Lambda_e$  that relate the mean free path of the convective elements to the local pressure scale height,  $H_P$ , for core and envelope overshoot, respectively.

It is worth recalling that in the convective cores,  $\Lambda_c$  is supposed to vary with the mass range. In brief, from the analysis of the CMDs and the LF of selected old open clusters (Aparicio et al. 1990; Bertelli et al. 1992; Carraro et al. 1993) the value  $\Lambda_c \simeq 0.25$  seems the more appropriate in the mass range  $1.0 M_\odot \leq M \leq 1.5 M_\odot$ . In the range

$1.6 M_{\odot} \leq M \leq 20 M_{\odot}$   $\Lambda_c$  is increased to 0.5 as suggested by pulsational properties of Cepheid stars of LMC clusters besides the CMDs and LF's of intermediate age and young clusters (Vallenari et al. 1991; Chiosi et al. 1992; Bertelli et al. 1992). Finally, in the range of massive stars (above  $20 M_{\odot}$ ) the value  $\Lambda_c \simeq 0.5$  is adopted. However, in this range of mass the evolution is so deeply dominated by mass loss that the effects of overshoot become negligible.

We remind the reader that  $\Lambda_c \simeq 0.5$  in the formalism of Bressan et al. (1981) corresponds to about the maximum overshoot distance advocated by Stothers (1991) or the overshoot distance favoured by Maeder & Meynet (1991) and Schaller et al. (1992).

As far as envelope overshoot is concerned (Alongi et al. 1991), a value  $\Lambda_e = 0.7$  is adopted as able to remove a number of discrepancies between theory and observations.

Finally, the mixing length parameter in the outermost super-adiabatic convective region of the envelope is  $1.63 \times H_P$ , so that the model with solar chemical composition and age can fit luminosity and effective temperature of the Sun. This means that these databases of stellar models and accompanying isochrones constitute calibrated sets of theoretical data suited to studies of population synthesis (cf. Bressan et al. 1993b).

## 2.2. Mass loss by stellar wind

Mass loss by stellar wind cannot be neglected in massive stars (Chiosi & Maeder 1986 and Chiosi et al. 1992). Therefore, for stars with initial mass between  $12 M_{\odot}$  and  $120 M_{\odot}$  the evolutionary models are computed taking into account mass loss according to the rates by de Jager et al. (1988) from the main sequence up to the so-called de Jager limit in the HRD. The rates also include the dependence on metallicity by Kudritzski et al. (1989). Beyond the de Jager limit the mass-loss rate is increased to  $10^{-3} M_{\odot} \text{ yr}^{-1}$  as suggested by observations of Luminous Blue Variables (LBV). For Wolf-Rayet stars the rates are according to Langer (1989).

Although significant mass loss by stellar wind may occur during the RGB and AGB phases, models of low and intermediate mass stars are computed at constant mass. How the models are handled to get the isochrones, taking into account mass loss in these late phases, will be described in more detail in next section.

## 2.3. Chemical elements, nuclear reaction rates and neutrino losses

For the solar metallicity the initial abundance of the elements heavier than helium is taken from Grevesse (1991). At varying metallicity, the initial abundances of these elements are changed however keeping their relative proportions as in the Grevesse (1991) compilation. In all cases, care has been paid to secure that the abundances are the

same as in the computations of the radiative opacities. The reference solar metallicity is  $Z_{\odot} = 0.020$ .

Nuclear energy generation rates are from Caughlan & Fowler (1988) including the  $^{12}\text{C}(\alpha, \gamma)^{16}\text{O}$  reaction in the He-burning phase, which is lower than estimated by Kettner et al. (1982), Langanke & Koonin (1982) and Caughlan et al. (1985). Schaller et al. (1992) adopted the higher rate by Caughlan et al. (1985) for the  $^{12}\text{C}(\alpha, \gamma)^{16}\text{O}$  reaction, and the effects show up in the He-burning phase, and in particular for the extension of the blue loops. This is one of the most noticeable differences in the input physics between the models used in this paper and those computed by the Geneva group.

The rates of neutrino emissions are from Munakata et al. (1985).

## 2.4. Opacities

Radiative opacities are from Iglesias et al. (1992) including the spin-orbit interaction in the treatment of Fe atomic data and the solar photospheric Fe abundance by Grevesse (1991) and Hannaford et al. (1992). An important improvement of the new opacity tabulations, with respect to the LAOL (Huebner et al. 1977) is given by the finer grid adopted in the temperature-density plane, which permits a better accuracy in the interpolation technique.

As OPAL tables do not extend below 6000 K and above  $10^8$  K, the opacities at lower and higher temperatures are taken from Huebner et al. (1977) and Cox & Stewart (1970a,b).

Finally, the contribution to the opacity by the CN, CO,  $\text{H}_2\text{O}$  and  $\text{TiO}$  molecules is included by means of the analytical relationships by Bessell et al. (1989, 1991), based on the tabulations by Alexander (1975) and Alexander et al. (1983).

## 2.5. Main characteristics of the evolutionary models

As the chemical compositions range from very low ( $Z=0.0004$ ) to high metal content ( $Z=0.05$ ), it is worth summarizing here the properties of the models that depend on metallicity. Increasing the metal content from the lowest to the highest value on consideration:

- a) the transition mass from low to intermediate mass stars firstly increases and then decreases ranging from  $M_{\text{HeF}} = 1.7 M_{\odot}$  to  $M_{\text{HeF}} = 2.0 M_{\odot}$ ;
- b) the lower mass on the main sequence for a star to possess a convective core is not monotonically related to the chemical composition; for  $Z=0.0004$  this mass is  $0.9 M_{\odot}$ , for  $Z=0.02$  is  $1.0 M_{\odot}$ , and for  $Z=0.05$  is  $0.8 M_{\odot}$ ;
- c)  $M_{\text{UP}}$ , the transition mass from intermediate to massive stars, is about  $5 M_{\odot}$  for all chemical compositions;
- d) the main sequence band gets cooler and widens significantly;
- e) the range of effective temperatures ( $T_{\text{eff}}$ ) covered by the



sub giant branches (SGB) decreases;  
f) the RGBs become more tilted toward lower  $T_{\text{eff}}$ s.

### 3. Technique of isochrone calculation

Isochrones are constructed by means of the same procedure as described in Bertelli et al. (1990) and as used to construct synthetic HRDs and integrated magnitudes and colors for star clusters (Chiosi et al. 1989a,b). Therefore, the discussion below is limited to a few key points.

Towards the tip of RGB of low mass stars, and during the AGB evolution of low and intermediate mass stars, the effects of mass loss by stellar wind must be included. The rate of mass loss is expressed by means of the empirical formulation by Reimers (1975), which in terms of the stellar mass, luminosity and effective temperature can be written as

$$\dot{M} = 1.27 \cdot 10^{-5} \eta M^{-1} L^{1.5} T_{\text{eff}}^{-2} \quad (M_{\odot}/\text{yr}) \quad (1)$$

where  $\dot{M}$ , and  $M, L$  are in solar masses per year and in solar units, respectively. The parameter  $\eta$  is assumed equal to 0.35 for low mass stars, and gradually increased up to  $\eta=1$  for intermediate mass stars, as indicated by the mass-loss rates of de Jager et al. (1988).

Passing from the tip of the RGB to the ZAHB, the inclusion of mass loss is a trivial affair. Because of the negligible effects of mass loss on the internal structure of model stars at the tip of the RGB, mass-loss can be applied to constant mass evolutionary tracks and reduced to simply scaling the mass down to the value suited to the ZAHB stars. This is achieved by integrating the mass-loss rate along the RGB to estimate the total amount of mass that has to be removed and to establish the relationship between the initial and ZAHB mass,  $M_i$  and  $M_{\text{HB}}$  respectively:

$$M_{\text{HB}} \equiv M_{\text{HB}}(M_i, \eta) \quad (2)$$

The inclusion of mass loss during the AGB phase is a more cumbersome affair. While, it can be neglected during the so-called early AGB phase (i.e. before the onset of the TP-AGB), mass loss is the key parameter to follow the evolution during the TP-AGB. The procedure to be adopted depends on the metallicity.

For all stellar sequences that in virtue of the metallicity have a regular AGB phase, the evolutionary tracks and corresponding isochrones are extended beyond the start of the TP-AGB and followed up to the stage of envelope ejection and termination of the TP-AGB regime in simple analytical fashion (see Renzini 1977; Iben & Renzini 1983; Bertelli et al. 1990 and Grönevege & de Jong 1993 for all details). The stellar model calculations by Alongi et al. (1993), Bressan et al. (1993a) and Fagotto et al. (1994a,b) show that the AGB phase is regular if the metallicity is below a certain value that can be set at about  $Z=0.05$ . To include mass loss, four basic relations are required, namely

the mass-loss rate of stellar wind, the relation connecting the mass of the H-exhausted core with the total luminosity of the star, the evolutionary rate at which the mass of the H-exhausted core grows under the action of the H-burning shell, and finally a suitable relation between the luminosity and the effective temperature while the star is climbing the AGB. In this paper we adopt core mass-luminosity relationship from the models by Boothroyd & Sackmann (1988), the mass loss rate of Eq. (1) with the parameter  $\eta$  increasing with the stellar mass, and a luminosity-effective temperature relation obtained by extrapolating the slope of the early AGB phase of our models to higher luminosities and lower effective temperatures.

In those cases in which the high metallicity destroys the regular behaviour of the AGB phase giving rise to the so-called AGB-manqué scheme (see Greggio & Renzini 1990; Bressan et al. 1993b; Fagotto et al. 1993a,b for all details and referencing) the above scheme does no longer hold and detailed models must be calculated in presence of mass loss. With the metallicity in use this is limited to a few cases of the set with metallicity  $Z=0.05$ .

The terminal stage of the isochrones is different in relation to the age (final mass) and corresponds to a star whose final fate is a white dwarf (initial mass  $M_i \leq 5 M_{\odot}$ ), or explosive carbon ignition in a strongly electron degenerate core ( $5 M_{\odot} < M_i < M_{\text{UP}}$ ), or ignition of carbon in a mildly degenerate core ( $M_i > M_{\text{UP}}$ ). For these latter cases, core C-ignition is the last stage of the isochrones.

If the star evolves toward the white dwarf (WD) stage, the isochrones include also the evolutionary phases across the HRD while the object appears as the central star of a planetary nebula (CSPN). In this case, we derive a suitable relation between the initial mass and the mass of the CSPN, shortly indicated as  $M_{\text{cs}}$ ,

$$M_{\text{cs}} = M_{\text{cs}}(M_i, \eta) \quad (3)$$

and add this phase to the isochrones.

The evolutionary sequences for the CSPNs are either taken from Schönberner (1983) and Blöcker & Schönberner (1990) for  $M_{\text{cs}} = 0.546, 0.565, 0.605, 0.836 M_{\odot}$  or explicitly calculated for  $M_{\text{cs}} = 0.5167$  and  $0.646 M_{\odot}$ . All these models possess the same initial chemical composition, namely  $[Z=0.020, Y=0.28]$  and have the same initial stage taken at  $\text{Log } T_{\text{eff}} = 3.70$  (the short-lived part of the sequence between the tip of the AGB and this initial stage is neglected). The age of the stellar models in the CSPN stage is inclusive of the lifetime elapsed from the zero age main sequence up to the tip of the AGB.

As already mentioned, starting from the metallicity  $Z=0.05$  the lowest mass HB tracks depart from the regular scheme of the AGB phase and must be calculated explicitly. This happens for initial masses  $M_i = 0.50 M_{\odot}$ ,  $0.55 M_{\odot}$ , and  $0.60 M_{\odot}$ , to which masses of the central object of the PN phase  $M_{\text{cs}} = 0.495 M_{\odot}$ ,  $0.524 M_{\odot}$ , and  $0.543 M_{\odot}$  are associated (Fagotto et al. 1994a,b).

However, with the adopted mass-loss rates this behaviour starts to occur at ages older than  $20 \cdot 10^9$  yr.

#### 4. Conversion from theoretical to observational plane

Theoretical luminosities and effective temperatures along the isochrones are translated to magnitudes and colors using extensive tabulations of bolometric corrections (BC) and colors obtained from properly convolving the spectral energy distributions (SEDs) contained in the library of stellar spectra kindly made available by Kurucz (1992 private communication). This library contains SEDs over a wide range of gravities, effective temperatures and metallicities.

It is worth recalling that Kurucz (1992) SEDs are not accurate enough for M stars, as acknowledged by Kurucz himself (1992) and thoroughly discussed by Malagnini et al. (1992) looking at the systematic UV discrepancies between Kurucz models and the observations of low temperature stars ( $T_{\text{eff}} \leq 4000$  K). To cope with this drawback of the library, we have adopted empirical SEDs for the coolest stars as described below.

Furthermore, as sometimes the isochrones in the CMD reach regions of effective temperatures and gravities not included in the SED library or for the problems of Kurucz models at low temperatures, the library of SEDs has been extended both at high and low temperatures according to the suggestions by Bressan et al. (1993b) in their study of population synthesis in elliptical galaxies.

For stars with high  $T_{\text{eff}}$ , i.e. above 50,000 K, and independently of gravity and chemical composition we assign pure black-body spectra. Smoothing of the flux at the transition temperature is secured by properly scaling the flux. This implicitly allows for a certain dependence on the chemical composition.

For stars with  $T_{\text{eff}}$  lower than 4,000 K (K and M type stars), the extension of the spectral library is a more cumbersome affair (see Lancon & Rocca-Volmerange 1992). The following procedure is adopted:

i) Three catalogs of observational spectra for late type stars are used and their spectral distribution acquired and digitized with the aid of an automatic scanner (the resolution technique is fully adequate to our purposes): a) the spectra for M stars in the near infrared from 14,280 to 25,000 Å published by Lancon & Rocca-Volmerange (1992); b) the spectra of M giants in the galactic bulge by Terndrup et al. (1990, 1991) in the range 5,000 - 25,000 Å; c) finally, spectra for M0V-M5V and M0III-M6III stars in the range 3,000 Å to 10,000 Å. by Straizys & Sviderskiene (1972).

ii) The three samples are used to synthesize the spectra for dwarf stars up to M7 and for giant stars up to M8.5. Mounting of the spectra is performed as follows. The fluxes of each spectrum in the wavelength intervals 3,000 to 10,000 Å and 14,280 to 25,000 Å are scaled in

such a way that the color ( $V-K$ ) matches the corresponding observational value for the spectral type on consideration. The observational colors for giant stars are from Bessell & Brett (1988) and Terndrup et al. (1991). In the spectral region from 10,000 to 14,280 Å we use either the spectra by Terndrup et al. (1991) when available or an analytical quadratic interpolation imposing that the color ( $J-K$ ) matches that of the corresponding spectral type. The same source as for the ( $V-K$ ) color is taken also for the ( $J-K$ ) color. The spectra are finally extended to wavelengths shorter than 3,000 Å and longer than 25,000 Å, by means of a black body spectrum with the same temperature of the spectrum on consideration. Continuity of the fluxes at the border wavelengths is secured. M supergiants are assigned the same spectrum of giant stars of the same  $T_{\text{eff}}$ .

iii) But for the latest M types, each composite spectrum is assigned the effective temperature adopted by Lancon & Rocca-Volmerange (1992). For the latest M spectral types we adopt the Rigdway et al. (1980) scale of  $T_{\text{eff}}$ , because the effective temperatures used by Lancon & Rocca-Volmerange (1992) are too cool in comparison with observational determinations.

iv) Although it might seem that the metallicity dependence of our library of stellar tracks is wiped out by the method used to extend the Kurucz (1992) library toward low  $T_{\text{eff}}$ s, in reality this does not occur and the dependence on metallicity is implicitly taken into account. As a matter of fact, at increasing metallicity stellar models and isochrones tend to redden and to shift from one spectral type to another, and hence low effective temperatures and cool spectral types are most favoured by a high metal content. They are also possibly limited to the very latest stages of normal stars. Therefore, the basic dependence on the metallicity is secured by the natural behavior of the underlying tracks at varying metallicity. In addition to this, we should also consider that the latest spectral types contained in the Terndrup et al. (1991) list refer to stars in the Galactic Bulge, which most likely are also more metal rich than the corresponding stars in the solar vicinity, and thus an indirect dependence on the metallicity is automatically taken into account.

The response functions for the various pass-bands in which magnitudes and colors are generated are from the following sources: Buser & Kurucz (1978) for the *UBV* passbands, Bessell (1990) for the *R* and *I* Cousins passbands, and finally Bessell & Brett (1988) for the *JHK* passbands. If requested, isochrones can be produced for colors in the *UBVR IJKLMN* Johnson photometry with the pass-band response functions that are described in Lamla (1982).

In order to calculate the colors from the SEDs, these have been normalized as follows. First we select the SED that best matches the observational SED of Vega and then

impose that the computed colors match the observed colors (Kurucz 1992).

Finally, the zero point of the BCs is fixed by imposing that the BC for the Kurucz model of the Sun is -0.08 (Bessell 1983).

### 5. Electronic data base of isochrones

The complete grids of isochrones are stored in the electronic data base of Astronomy and Astrophysics at the Centre de Données Stellaires (CDS) in Strasbourg. The electronic catalog consists of Tables 1 to 6 each one corresponding to a different chemical composition indicated in the heading of the tables by the helium content  $Y$  and metallicity  $Z$ . Each isochrone is labelled by the age (logarithmic value in years) and the chemical parameters. In general, all isochrones whose terminal stage is the formation of WD stars, are split in three or two parts depending on whether they proceed through core He-flash or quiet core He-ignition. The various groups correspond to different evolutionary stages. In the first case, the three groups are: from the main sequence up to the tip of the RGB, core He-burning on the HB and whole AGB phase (shortly indicated as HB+AGB PHASE), and the evolution from the tip of AGB down to the WD regime (shortly indicated as P-AGB PHASE). In the second case, only the P-AGB phase is put into evidence. However, if the WD mass is greater than  $1 M_{\odot}$  the P-AGB phase is not calculated and only the WD mass is given. Finally, no distinction at all is made for those isochrones, whose final stage is either quiet or explosive C-ignition in the core.

For each isochrone the following quantities are listed: *Column 1 (MASS)*: the mass in solar units along the isochrone. This value of the mass corresponds to the current initial mass, except for the isochrones going through the core He-flash, as the mass after the tip of the RGB is decreased by the effect of mass loss. The same holds for the P-AGB stages. In these later stages the true initial mass is not tabulated, but it can be easily calculated by inverting Eq. (6) below. *Column 2 (LOGTE)*: the logarithm of the effective temperature. *Column 3 (MBOL)*: the bolometric magnitude. *Column 4 (MG V)*: the absolute visual magnitude in the Johnson system. *Column 5 to Column 11*: the colors ( $U - B$ ), ( $B - V$ ), ( $V - R$ ), ( $V - I$ ), ( $V - J$ ), ( $V - H$ ), ( $V - K$ ) as described in the previous section. *Column 12 (FLUM)*: the indefinite integral of the initial mass function by number over the mass

$$FLUM = \int \Phi(M) dM. \quad (4)$$

This is calculated assuming the Salpeter law

$$\Phi(M) = A \cdot M^{-\alpha} \quad (5)$$

with  $\alpha = 2.35$  and the normalization constant  $A=1$ , so that

$$FLUM = \frac{M^{1-\alpha}}{1-\alpha} \quad (6)$$

where  $M$  is the initial mass associated to the current mass along the isochrone. The difference between any two values of  $FLUM$  is proportional to the number of stars born in the corresponding mass interval, whereas the ratio between any two differences gives the relative number of stars in the corresponding phases. When mass loss occurs (transition from RGB to HB and TP-AGB phase),  $FLUM$  is always computed in terms of the initial stellar mass with the aid of the relationships between the initial and current mass.

At certain characteristic stages of each isochrone we display the integrated  $V$ ,  $K$  and bolometric magnitudes (IMV, IMK, and Mb) and the integrated colors ( $U - B$ ,  $B - V$ ,  $V - R$ ,  $V - I$ ,  $V - J$ ,  $V - H$ , and  $V - K$ ). In spite of the identical notation, the integrated colors can be easily distinguished from the current values of the corresponding quantities along the isochrone, because of the different layout.

Magnitudes and colors are computed summing up the fluxes from each mass interval in the proper pass-band and weighting them on the initial mass function (Searle et al. 1973):

$$F_{\Delta\lambda} = \sum A\Phi(M_i)10^{-0.4M_{\Delta\lambda}(M_i)}\Delta M_i \quad (7)$$

where  $F_{\Delta\lambda}$  is the integrated flux at the characteristic wavelength,  $M_i$  is the initial star mass,  $M_{\Delta\lambda}(M_i)$  is the magnitude in the same pass-band corresponding to the mass  $M_i$  along the isochrone. The summation extends from the beginning of the isochrone to the point under consideration, assuming the normalization constant of the initial mass function  $A = 1$ . From this definition of the integrated flux, the integrated magnitudes follow immediately from

$$M_{\Delta\lambda} = -2.5 \text{ Log } F_{\Delta\lambda} \quad (8)$$

The integrated absolute magnitudes of real clusters can be obtained by suitably scaling the normalization constant  $A$  to the value appropriate for the total number of stars in the clusters under consideration.

At the end of each isochrone, we give the final mass of the star according to the cases: i) the mass of the WD named  $M_{WD}$  for isochrones encompassing the complete evolution down to the WD formation; ii) the Chandrasekhar mass of the core, named  $M_c = 1.4 M_{\odot}$  when C-burning ignites explosively. No final mass is given for all the isochrones terminating with quiet carbon ignition.

For the youngest isochrones, whose evolved part corresponds to masses for which mass loss by stellar wind is very efficient, the column ( $V - K$ ) is dropped and in the last column we display the real value of the mass along the isochrone. This mass is named  $M_{wind}$ . Noteworthy, the mass  $M_{wind}$  is much different from that in Col. (1) now simply indicating the mass of the underlying evolutionary sequence from which the isochrones are derived. Because of the ongoing mass loss in the course of a massive star



evolution, along the isochrone the mass continuously decreases, contrary to what happens in the case of constant mass evolution where the mass increases as a result of the increasing evolutionary rate.

Finally, for the sake of illustration, in the series of Figs. 1 through 6 we present a few selected isochrones for the six chemical compositions as indicated. Panels (a) show isochrones for ages in the range  $6.6 < \log T < 9.0$ , whereas panels (b) show isochrones for ages going from  $\log T = 9.2$  to  $\log T = 10.2$ .

## 6. Summary tables of the isochrone grids

In order to facilitate the use of our isochrone tabulations, in the series of Tables 7 through 12 and Figs. 7 through 13, we present a summary of the most significant stages of the isochrone for each chemical composition. The characteristic stages are:

- a) The turnoff (TO), i.e. the bluest point during core H-burning.
- b) The reddest point before the overall contraction phase at the end of the core H-burning (indicated as stage B).
- c) The stage of core H-exhaustion (indicated as stage C).
- d) The base of the RGB ( $B_{\text{RGB}}$ ).
- e) The tip of the RGB ( $T_{\text{RGB}}$ ).
- f) The mean locus of the core-He burning phase ( $M_{\text{Heb}}$ ). This is evaluated graphically, plotting the luminosity (or  $M_V$ ) versus the current mass along the isochrone.
- g) The bluest stage during core He-burning in presence of a loop ( $B_{\text{Heb}}$ ).
- h) The reddest stage during core He-burning in presence of a loop ( $R_{\text{Heb}}$ ).
- i) The tip of the AGB ( $T_{\text{AGB}}$ ).
- j) Finally, the last computed model (LM) for all cases in which the AGB phase does not occur.

The layout of the Tables 7 through 12 is as follows: Column 1 (Age): the logarithm of the age in yr; Column 2 (Phase): the characteristic stage; Column 3 ( $M$ ): the current mass in solar units; Column 4 ( $T_{\text{eff}}$ ): the logarithm of the effective temperature; Column 5 ( $L$ ) the logarithm of the luminosity in solar units; Column 6 ( $M_V$ ): the absolute visual magnitude; Columns 7, 8, 9, and 10: the colors ( $B - V$ ), ( $V - I$ ), ( $V - J$ ), and ( $V - K$ ), respectively.

### 6.1. Main sequence

Figures 7, 8, and 9 show the three classical age indicators based on the core H-burning phase, i.e. the turn-off, the stage of lowest  $T_{\text{eff}}$  (stage B), and the stage of core H-exhaustion or equivalently of brightest luminosity (stage C), respectively. As expected, all the three characteristic points are good indicators of the age provided that a hint on the chemical composition is available. On the average, ignoring the chemical composition introduces an uncertainty in the age of about  $\Delta \log T = 0.2$ . The relation between the absolute magnitude and age for the turn-off

shows a dip at about  $\log T = 9.4$  yr which corresponds to the transition from radiative to convective core H-burning and consequent change of the isochrone shape (see Figs. 1 through 6).

### 6.2. Red giant branch and He-burners

The luminosity (magnitude  $M_V$ ) of the bottom of the RGB is known to depend on the age and chemical composition (metallicity). This is shown in Fig. 10. Up to ages of about  $\log T = 9.3$  yr, the slope of the relation is such that ignoring the metallicity yields an uncertainty in the age of about  $\Delta \log T = 0.35$  when the composition varies from  $[Z=0.0004, Y=0.230]$  to  $[Z=0.05, Y=0.352]$ . Beyond this stage the relation flattens out and the uncertainty gets larger. To be used as an age indicator, the above relation must be supplemented by information on the chemical composition.

The luminosity (magnitude  $M_V$ ) at the tip of the RGB as a function of the age and chemical composition is shown in Fig. 11. Before the onset of strong electron degeneracy in the He-core and consequent appearance of well developed RGBs, but for the case with the highest metallicity and helium content, the relation primarily depends on the age so that neglecting the information on the chemical composition is less of a problem. Therefore good ages can be estimated over a large range going from about  $\log T = 7.8$  yr to about  $\log T = 8.9$  yr. Beyond this value of the age, either the relation becomes flat (as for metallicities up to  $Z=0.001$ , namely the range typical of globular clusters) or decreases at increasing age and metallicity.

The magnitude  $M_V$  of the mean locus of stationary core He-burners is shown in Fig. 12 for the six chemical compositions. As expected at increasing age it gets fainter as long as the underlying stars do not undergo core He-flash, whereas it is about constant when the stars suffer core He-flash.

In the first mass range, the dependence on the chemical composition is strong and together with the varying extension of the blue loops in the HRD destroys the regular behaviour of the relation between luminosity and age that can be inferred from the data of Tables 7 to 12.

In the lower mass range, the dependence on the chemical composition of core He-burners is slightly more complex. We start with the general relation between the metallicity  $Z$  and the iron content  $[\text{Fe}/\text{H}]$

$$\log Z = \log(X/X_{\odot}) + \log Z_{\odot} + [\text{Fe}/\text{H}] \quad (9)$$

where  $X$  is the hydrogen content and all the symbols have their usual meaning. For the solar values we assume  $X_{\odot} = 0.70$  and  $Z_{\odot} = 0.020$ . The ratio  $X/X_{\odot}$  varies with the metallicity  $Z$  according to the enrichment ratio  $\Delta Y/\Delta Z$ . Expressing the ratio  $X/X_{\odot}$  as a function of  $\log Z$  we get

$$\text{Log } Z = 0.977[\text{Fe}/\text{H}] - 1.699 \quad (10)$$

or conversely

$$[\text{Fe}/\text{H}] = 1.024 \log Z + 1.739 \quad (11)$$

With the aid of the above equations, we derive the following relation for the  $M_V$  of the HB stars as function of the metallicity and age

$$M_V = 0.147[\text{Fe}/\text{H}] + 0.62 \log T_9 + 0.173 \quad (12)$$

where  $T_9$  is the age in units of  $10^9$  yr. This relation can be safely applied in the metallicity and age ranges  $0.0004 < Z < 0.008$  and  $10.0 < \log T < 10.2$  yr, respectively.

The observational  $M_V - [\text{Fe}/\text{H}]$  relation determined by Sandage (1993a,b, and references therein) studying the Oosterhoff effect is

$$M_V = 0.30[\text{Fe}/\text{H}] + 0.94 \quad (13)$$

While for a typical age of globular clusters of  $15 \cdot 10^9$  yr the zero point of the theoretical relation agrees with that of the empirical one, the slopes are different. We would like to point out that the slope we have obtained is similar to that from the classical models by Sweigart et al. (1987) and Lee (1990). The many implications arising from the adoption of a certain  $M_V - [\text{Fe}/\text{H}]$  relation to study the CMD of globular clusters have been thoroughly reviewed by Renzini & Fusi-Pecchi (1988), Chiosi et al. (1992), Fusi-Pecchi & Cacciari (1991), and Sandage (1993a,b) to whom the reader should refer for all details.

One of the most popular methods to date globular clusters rests on the difference between the turn-off and the HB magnitudes,  $\Delta M_V^{\text{TO}}$  (see Chiosi et al. 1992). The data of Tables 7 to 12 can be approximated by the analytical fit

$$\Delta M_V^{\text{TO}} = 1.5 \log T_9 + 0.234[\text{Fe}/\text{H}] + 2.062 \quad (14)$$

where the dependence on the helium content is implicitly taken into account. The above relation can be safely used if ages and metallicity are in the range  $10.0 < \log T < 10.2$  yr and  $-2 < [\text{Fe}/\text{H}] < -0.5$ , respectively. On the observational side,  $\Delta M_V^{\text{TO}} = 3.54$  (Buonanno et al. 1989). Inserting this value in the above equation and assuming  $Z=0.001$  ( $[\text{Fe}/\text{H}] = -1.33$ ) for the metallicity of the bulk of globular clusters we get an age of  $15.6 \cdot 10^9$  yr, in agreement with current estimates (cf. Sandage 1993b). A deeper analysis of this topic is beyond the present aims.

We remind the reader that in all the above theoretical relations the dependence on the helium content  $Y$  does not explicitly appear because the data in Tables 7 through 12 are based on stellar models that already include the dependence  $\Delta Y/\Delta Z = 2.5$ .

### 6.3. Maximum AGB luminosity

The luminosity at the tip of the AGB phase of low and intermediate mass stars provides another age indicator that is particularly useful in those cases in which only the brightest stars are observed (Iben & Renzini 1983). This method has been widely used to infer the age of bright red stars (most probably AGB stars) in nearby galaxies for which a CMD down to the turn-off luminosity is not yet feasible. A typical example is provided by the CMDs of M32 obtained by Freedman (1989, 1992), Elston & Silva (1992), and Davidge & Jones (1992). The existence of bright objects was considered as indicating an episode of star formation as recent as  $5 \cdot 10^9$  yr ago. The analysis was however hampered by the limitations in the calibrating relationships (maximum luminosities as a function of the age and chemical composition). Indeed most of the calibrations in usage refer to the solar composition. Bressan et al. (1993b) re-examining the nature of the bright stars in M32 presented new calibrations for the  $V$ ,  $I$  and  $K$  pass-bands based on the present library of isochrones. They found that in the  $I$  versus  $(V - I)$  CMD the maximum AGB luminosity is a sensitive function both of the age and metallicity, whereas in the  $K$  versus  $(J - K)$  CMD only the age plays the key role. In particular, they found that in the  $I$  versus  $(V - I)$  CMD high-metallicity, young AGB stars can be hardly distinguished from low-metallicity, old AGB stars. On the contrary, in the  $K$  versus  $(J - K)$  CMD a young AGB star is definitely more luminous than an old one and the metallicity is less of a problem. This means that age and metallicity effects can be singled out. The results presented by Bressan et al. (1993b) can be easily recovered from the data contained in Tables 7 through 12. In this paper, we present the calibration for the maximum luminosity attainable by AGB stars limited to the  $V$  pass-band. This is shown in Fig. 13, where the enormous effect due to the chemical composition is evident. Similar trends occur for the  $B$  pass-band. This means that with the standard  $BV$  photometry, reliable information on the age of the brightest AGB stars cannot be obtained without specifying their chemical composition. Magnitudes and colors in the near infrared ought to be preferred.

### 7. Initial - final mass relationship

Although a thorough discussion of the Initial-Final Mass Relationship  $M_f(M_i)$  is beyond the scope of this paper, it is worth comparing the  $M_f(M_i)$  resulting from our isochrone calculations with that by Vassiliadis & Wood (1993) and the popular, empirical relation derived long ago by Weidemann (1987).

This is shown in Fig. 14, in which both the theoretical and empirical relations are displayed. The theoretical  $M_f(M_i)$  relations are limited to the cases with metallicity  $Z=0.008$ . The  $M_f(M_i)$  of our models for other chemical compositions can be derived from the electronic database



(Tables 1 through 6). Filled circles and squares show the  $M_f(M_i)$  from Vassiliadis & Wood (1993) and from our isochrones, respectively. The open symbols indicate the relation between the initial mass and the core mass at the start of the TP-AGB phase. The most significant differences between our models and those by Vassiliadis & Wood (1993) are the mild overshoot in the former and the much more efficient mass-loss rate at increasing mass and the use of the LAOL opacity in the latter. The following remarks can be made:

- 1) The theoretical relations at the start of the TP-AGB phase agree for initial masses lighter than about  $3 M_\odot$ , whereas above it our relation is steeper than in Vassiliadis & Wood (1993). This can be ascribed to the effect of mild overshoot present in our models. At given initial mass, the mass of the H-exhausted core at this stage is bigger than in models in which convective overshoot is neglected.
- 2) The theoretical relations at the start of the TP-AGB phase run first below (for  $M_i < 3 M_\odot$ ) and then above (for  $M_i > 3 M_\odot$ ) the empirical one by Weidemann (1987). If the trend below  $3 M_\odot$  can be explained by the fact that the core has not yet grown to the size pertinent to the AGB tip, the trend above  $3 M_\odot$  simply indicates that convective overshoot cannot be the cause, because also models with the classical convective scheme lie above the empirical relation.
- 3) Finally, both theoretical  $M_f(M_i)$  relations run above the empirical one.

To a certain extent, the disagreement between the empirical and theoretical  $M_f(M_i)$  is less of a problem, since the final  $M_f(M_i)$  depends on the efficiency of mass loss and the underlying core mass-luminosity relation, whereas the disagreement with the Weidemann (1987) relation already at the start of the TP-AGB phase is a more cumbersome affair as any modification to the relation between the core and the initial mass of the star would imply severe changes both in the input physics and model structure in the previous evolutionary phases. In this context we would like to notice that i) the above disagreement occurs independently of the metallicity (cf. Tables 1 through 6, ii) it starts above  $3 M_\odot$  which almost coincides with the minimum mass for a star to undergo the second dredge up. Recalling that the core mass at the beginning of the TP-AGB phase results from the competition between the outward displacement of the He-burning shell and the inward penetration of the external convection, a possible way out could be a more efficient penetration of the external convection halting earlier the growth of the core. Among others this could be caused by higher opacities, different treatment of external convection, more efficient envelope overshoot, etc.

Furthermore, considering the number of improvements in model calculations achieved over the last few years (in particular the effect of the new radiative opacities and extension of convective cores), another possibility is that

also the empirical relation requires some revision. Indeed this is not totally independent of stellar models as at least the initial mass is derived from comparing observational data with stellar model calculations.

The above discussion clearly indicates that the problem of the correct  $M_f(M_i)$  is still far from being solved.

Since a deeper analysis of all the possible ways out to the difficulty in question is beyond the scope of this paper, we conclude this section telling the reader how to change the  $M_f(M_i)$  predicted by our isochrones on the basis of his/her favourite mass-loss rate and core mass-luminosity relation. No such possibility exists for the core mass-initial mass relation at the start of the TP-AGB phase without changing the library of stellar models we have adopted to calculate the isochrones.

Tables 1 through 6 of the electronic database, in coincidence with the start of the TP-AGB phase, display the core mass and the current star mass ( $M_{\text{cur}}$ ) at this stage. With the aid of these quantities and the current values of the luminosity, mass,  $T_{\text{eff}}$ , etc. the TP-AGB phase can be re-calculated and the new  $M_f(M_i)$  derived for different assumptions concerning the core mass-luminosity relation and mass loss rates. Finally, with the aid of the precepts by Renzini & Buzzoni (1983) for the evolutionary flux of single stellar populations, the P-AGB phase can be assigned to each isochrone.

## 8. Concluding remarks

The isochrones presented in this paper have been already used to interpret the CMDs and luminosity functions of a few young, rich clusters of the LMC, like NGC 2134 and NGC 2249 (Vallenari et al. 1994a), and of active star formation regions as NGC 1850 and NGC 1858 (Vallenari et al. 1994b) for the determination of the age, metallicity, and slope of the initial mass functions of these clusters. Furthermore, this library of isochrones has been at the base of the study of population synthesis and spectro-photometric evolution of elliptical galaxies by Bressan et al. (1993b), in which among other topics a detailed analysis of the nature of UV-excess in these systems has been presented.

*Acknowledgements.* This work has been financially supported by the Ministry of University and Scientific and Technological Research (MURST), and the Italian Space Agency (ASI).

## References

- Alexander D.R. 1975, ApJS 29, 363
- Alexander D.R., Johnson H.R., Ryma R.L. 1983, ApJ 272, 773
- Alongi M., Bertelli G., Bressan A., Chiosi C. 1991, A&A 244, 95
- Alongi M., Bertelli G., Bressan A. et al. 1993, A&AS 97, 851

- Aparicio A., Bertelli G., Chiosi C., Garcia-Pelayo J.M. 1990, *A&A* 240, 262
- Bertelli G., Betto R., Bressan A. et al. 1990, *A&AS* 85, 845
- Bertelli G., Bressan A., Chiosi C. 1992, *ApJ* 392, 522
- Bessell M.S. 1983, *PASP* 95, 480
- Bessell M.S. 1990, *PASP* 102, 1181
- Bessell M.S., Brett J.M. 1988, *PASP* 100, 1134
- Bessell M.S., Brett J.M., Scholz M., Wood P.R. 1989, *A&AS* 77, 1
- Bessell M.S., Brett J.M., Scholz M., Wood P.R. 1991, *A&AS* 87, 621
- Blöcker T., Schönberner D. 1990, *A&A* 240, L11
- Blöcker T., Schönberner D. 1991, *A&A* 244, L43
- Boothroyd A.I., Sackmann I.-J. 1988, *ApJ* 328, 671
- Bressan A., Bertelli C., Chiosi C. 1981, *A&A* 102, 25
- Bressan A., Fagotto F., Bertelli G., Chiosi C. 1993a, *A&AS* 100, 647
- Bressan A., Chiosi C., Fagotto F. 1993b, *ApJS*, in press
- Buonanno R., Corsi C.E., Fusi-Pecchi F. 1989, *A&A* 216, 80
- Buser R., Kurucz R.L. 1978, *A&A* 70, 555
- Canuto V., Mazzitelli I. 1991, *ApJ* 370, 295
- Carraro G., Bertelli G., Bressan A., Chiosi C. 1993, *A&AS* 101, 381
- Cattaneo F., Brummel N.H., Toomre J., Lalagoli A., Hurburt N.E. 1991, *ApJ* 370, 282
- Caughlan G.R., Fowler W.A. 1988, *Atomic Data Nucl. Data Tables* 40, 283
- Caughlan G.R., Fowler W.A., Harris M., Zimmermann B. 1985, *Atomic Data Nucl. Data Tables* 32, 197
- Charbonnel C., Meynet G., Maeder A., Schaller G., Schaerer D. 1993, *A&AS* 101, 415
- Chiosi C., Bertelli G., Bressan A. 1992, *ARA&A* 30, 305
- Chiosi C., Bertelli G., Meylan G., Ortolani S. 1989a, *A&AS* 78, 89
- Chiosi C., Bertelli G., Meylan G., Ortolani S. 1989b, *A&A* 219, 167
- Chiosi C., Maeder A. 1986, *ARA&A* 24, 239
- Cox A.N., Stewart J.N. 1970a, *ApJS* 19, 243
- Cox A.N., Stewart J.N. 1970b, *ApJS* 19, 261
- Davidge T.J., Jones J.H. 1992, *AJ* 104, 1365
- Elson R., Silva D.R. 1992, *AJ* 104, 1360
- Fagotto F., Bressan A., Bertelli G., Chiosi C. 1994a, *A&AS* 104, 365
- Fagotto F., Bressan A., Bertelli G., Chiosi C. 1994b, *A&AS*
- Freedman W.L. 1989, *AJ* 98, 1285
- Freedman W.L. 1992, *AJ* 104, 1349
- Fusi-Pecchi F., Cacciari C. 1991, in *New Windows to the Universe*, eds. F. Sanchez, A. Vasquez (Cambridge: Cambridge Univ Press) p. 364
- Greggio L., Renzini A. 1990, *ApJ* 364, 35
- Grevesse N. 1991, *A&A* 242, 488
- Groenewegen M.A.T., de Jong T. 1993, *A&A* 267, 410
- Gulati R.K., Malagnini M.L., Morossi C. 1993, *ApJ* 413, 166
- Hannaford P., Lowe R.M., Grevesse M., Noels A. 1992, *A&A* 259, 301
- Huebner W.F., Merts A.L., Magee N.H., Argo M.F. 1977, Los Alamos Scientific Laboratory Report LA-6760-M
- Iben I. Jr., Renzini A. 1983, *ARA&A* 21, 271
- Iglesias C.A., Rogers F.J., Wilson B.G. 1992, *ApJ* 397, 717
- de Jager C., Nieuwenhuijzen H., van der Hucht K.A. 1988, *A&AS* 72, 259
- Kettner K. U., Becker H. W., Buchmann L. et al. 1982, *Z. Phys.* 308, 73
- Kudritzski R.P., Pauldrach A., Puls J., Abbot D.C. 1989, *A&A* 219, 205
- Kurucz R.L. 1992, in *Stellar Populations of Galaxies*, eds. B. Barbuy and A. Renzini (Dordrecht: Kluwer) p. 225
- Lamla E. 1982, in *Landolt-Börnstein, New Series, Subvolume 2b, Stars and Star Clusters*, eds. K. Schaifers and H.H. Voigt (Berlin: Springer Verlag) p. 71
- Lancon A., Rocca-Volmerange B. 1992, *A&AS* 96, 593
- Langanke K., Koonin S.E. 1982, *Nucl. Phys.* A410, 334
- Langer N. 1989, *A&A* 210, 93
- Langer N. 1992, *A&A* 265, L17
- Lee Y.W. 1990, *ApJ* 363, 159
- Maeder A., Meynet G. 1991, *A&AS* 89, 451
- Malagnini M.L., Morossi C., Buser R., Parthasarathy M. 1992, *A&A* 261, 558
- Moskalik P., Buchler J.R., Marom A. 1992, *ApJ* 385, 685
- Munakata H., Kohyama Y., Itoh N. 1985, *ApJ* 296, 197
- Pagel B.E.J. 1989, in *Evolutionary Phenomena in Galaxies*, eds. J. Beckman and B.E.J. Pagel (Cambridge: Cambridge University Press) p. 201
- Reimers D. 1975, *Mem. Soc. R. Liège, Ser.6* 8, 369
- Renzini A. 1977, in *Advanced Stages of Stellar Evolution*, eds. P. Bouvier and A. Maeder (Geneva Observatory) p. 151
- Renzini A., Buzzoni A. 1983, *Mem. Soc. Astron. It.* 54, 379
- Renzini A., Fusi-Pecchi F. 1988 *ARA&A* 26, 199
- Rigdway S.T., Joyce R.R., White N.M., Wing R.F. 1980, *ApJ* 235, 126
- Rogers F.J., Iglesias C.A. 1992, *ApJS* 79, 507
- Sandage A. 1993a, *AJ* 106, 703
- Sandage A. 1993b, *AJ* 106, 719
- Schaerer D., Meynet G., Maeder A., Schaller G. 1993a, *A&AS* 98, 523
- Schaerer D., Charbonnel C., Meynet G., Maeder A., Schaller G. 1993b, *A&AS*, in press
- Schaller G., Schaerer D., Meynet G., Maeder A. 1992, *A&AS* 96, 269
- Schönberner D. 1983, *ApJ* 272, 708
- Searle L., Sargent L.W., Bagnuolo W.G. 1973, *ApJ* 239, 803
- Stothers R. 1991, *ApJ* 383, 820

- Stothers R., Chin C.W. 1991, ApJ 381, L67
- Straizys V., Sviderskiene Z. 1972, Bull. Vilnius Obs. Nr. 35, 3
- Sweigart A., Renzini A. Tornambé A. 1987, ApJ, 312, 762
- Terndrup D.M., Frogel J.A., Withford A.E. 1990, ApJ 357, 453
- Terndrup D.M., Frogel J.A., Withford A.E. 1991, ApJ 378, 742
- Vallenari A., Chiosi C., Bertelli G., Meylan G., Ortolani S. 1991, A&AS 87, 517
- Vallenari A., Chiosi C., Bertelli G., Meylan G., Ortolani S. 1992, AJ 104, 1100
- Vallenari A., Aparicio A., Fagotto F., Chiosi C. 1994a, A&A 284, 424
- Vallenari A., Aparicio A., Fagotto F., Chiosi C., Ortolani S., Meylan G. 1994b, A&A 284, 447
- Vassiliadis E., Wood P.R. 1993, ApJ 413, 641
- Weidemann V. 1987, A&A 188, 74
- Zahn J.P. 1991, A&A 252, 179



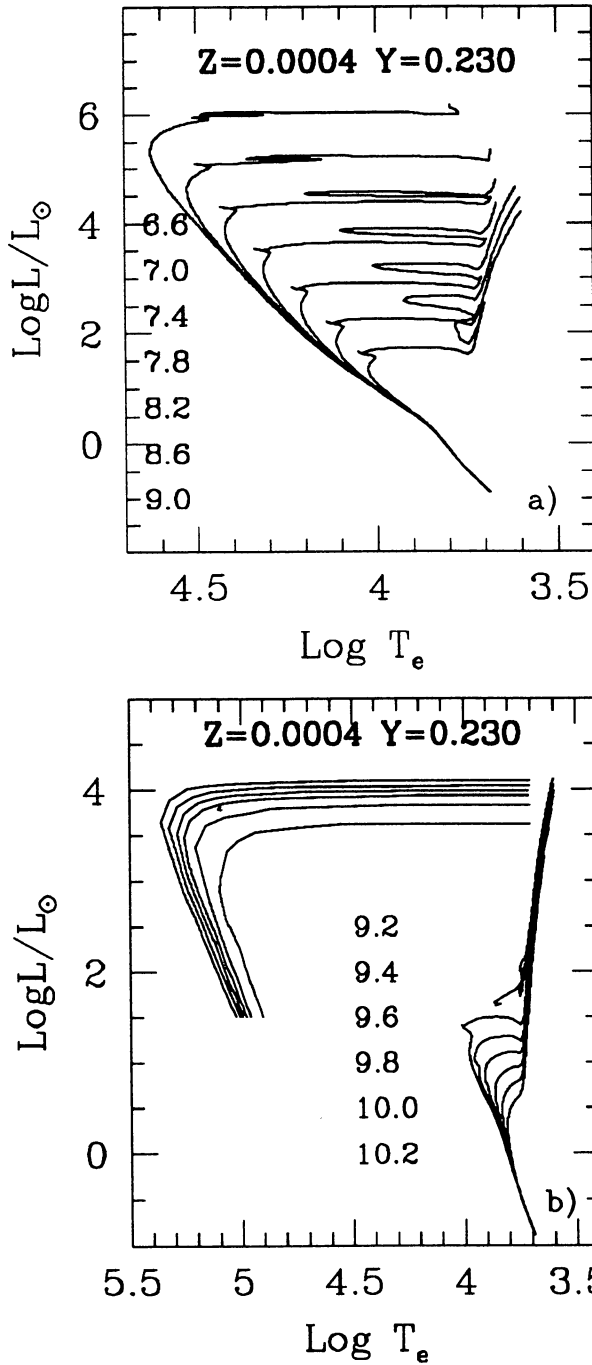


**Fig. 1.** Isochrones in the C-M diagram with initial chemical composition [ $Z=0.0004$ ,  $Y=0.230$ ] and mass-loss parameter  $\eta = 0.35$ . Panel (a) refers to isochrones with turn-off mass greater than  $M_{\text{HEF}}$ , whereas panel (b) refers to isochrones with turn-off mass lower than  $M_{\text{HEF}}$ . Ages (logarithmic value in years) are indicated in each panel. Limited to this case, we also show in panel (b) the part of the isochrones going from the tip of the AGB down to the WD cooling sequence

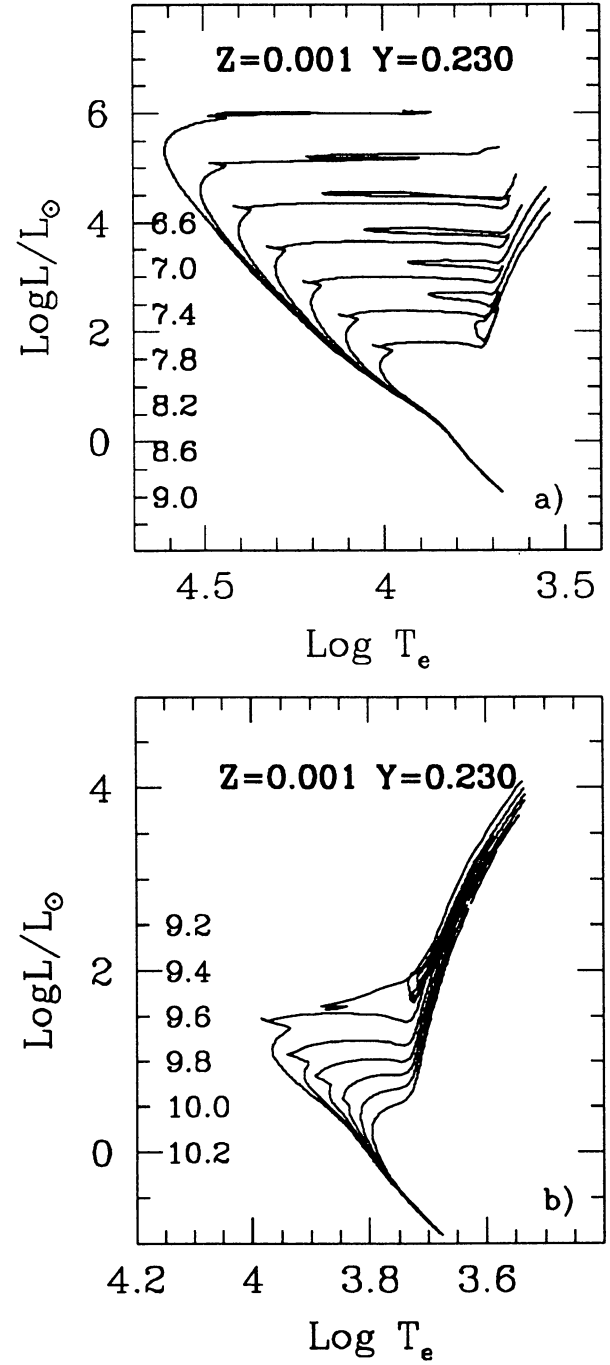


**Fig. 2.** The same as in Fig. 1, but for the composition [ $Z=0.001$ ,  $Y=0.230$ ]

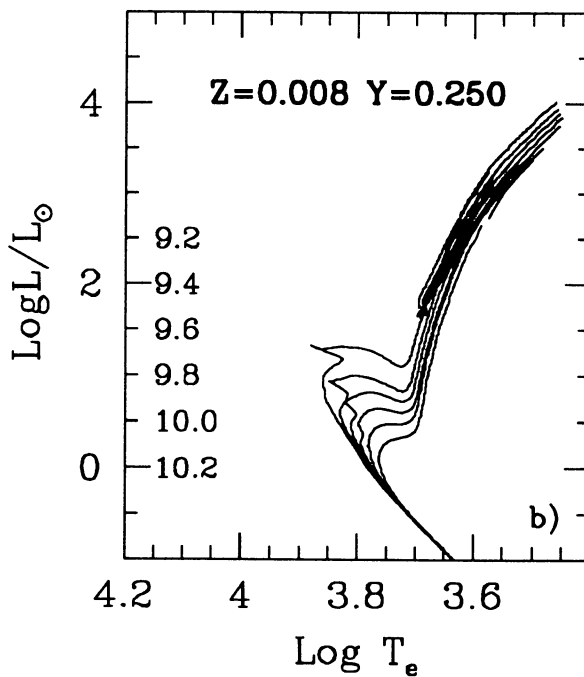
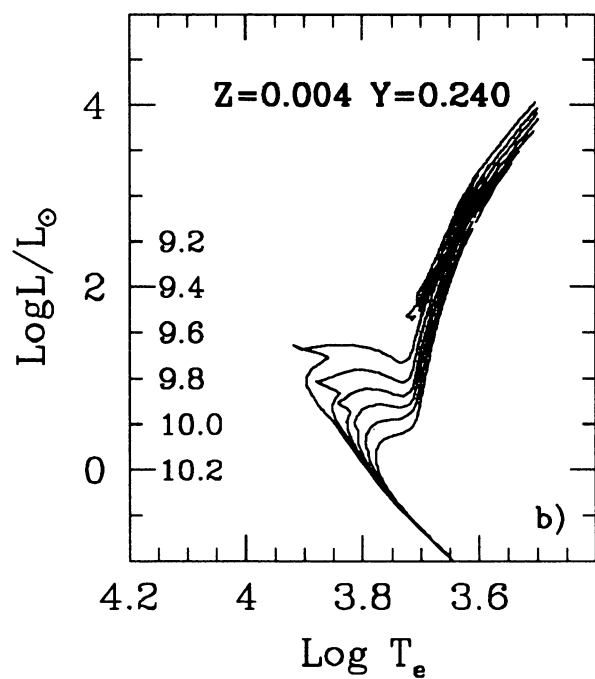
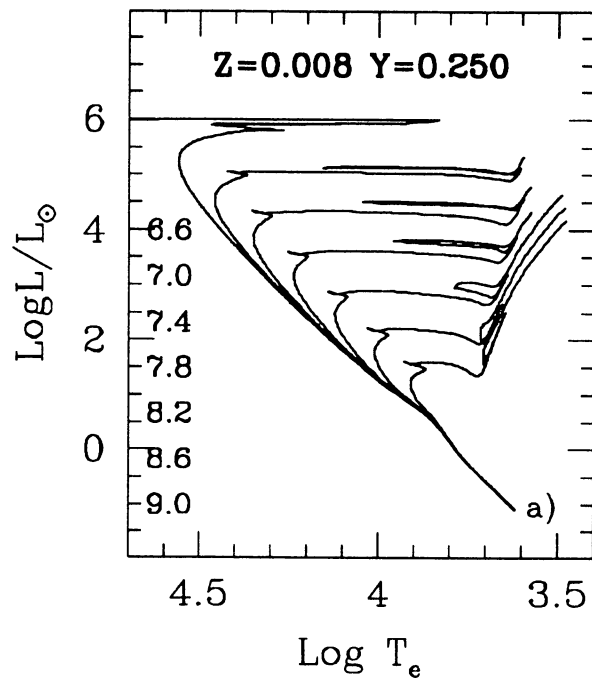
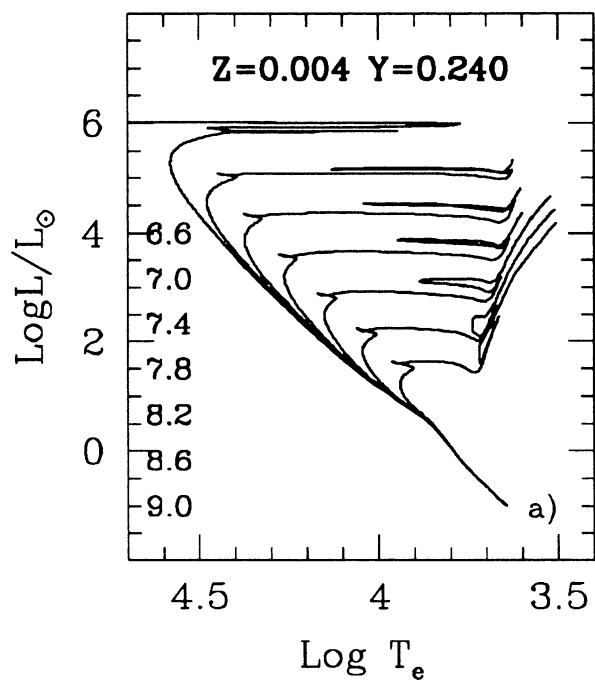


**Fig. 3.** The same as in Fig. 1, but for the composition  $[Z=0.004, Y=0.240]$

**Fig. 4.** The same as in Fig. 1, but for the composition  $[Z=0.008, Y=0.250]$

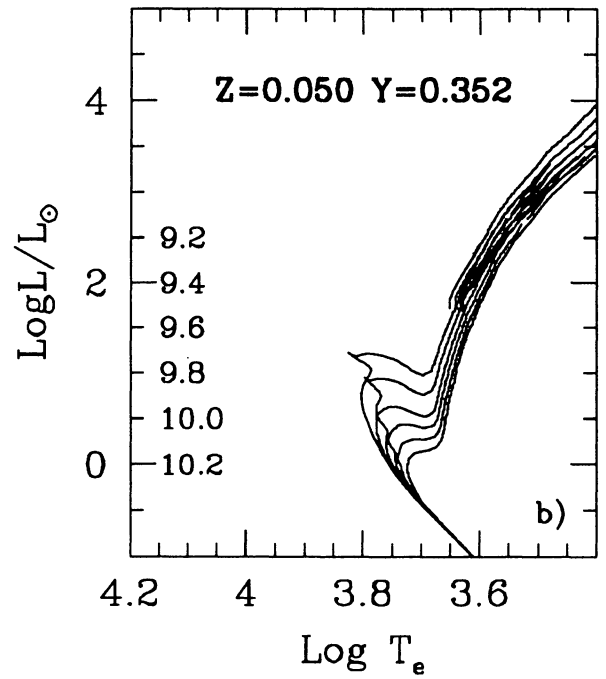
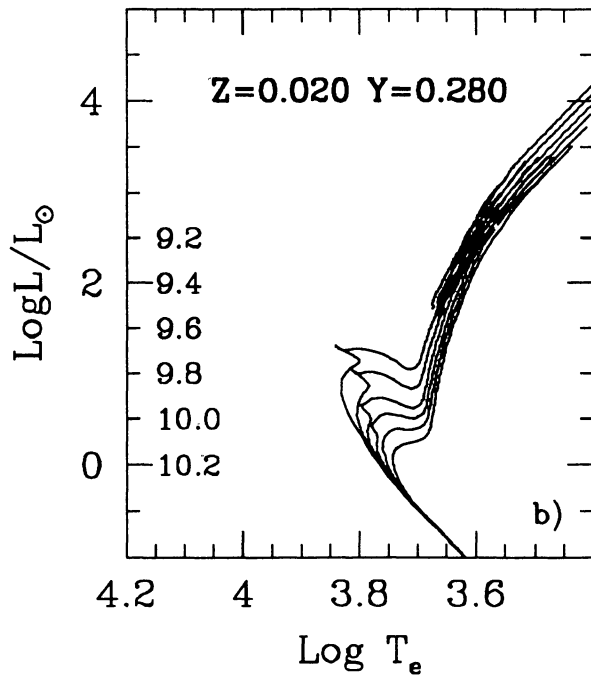
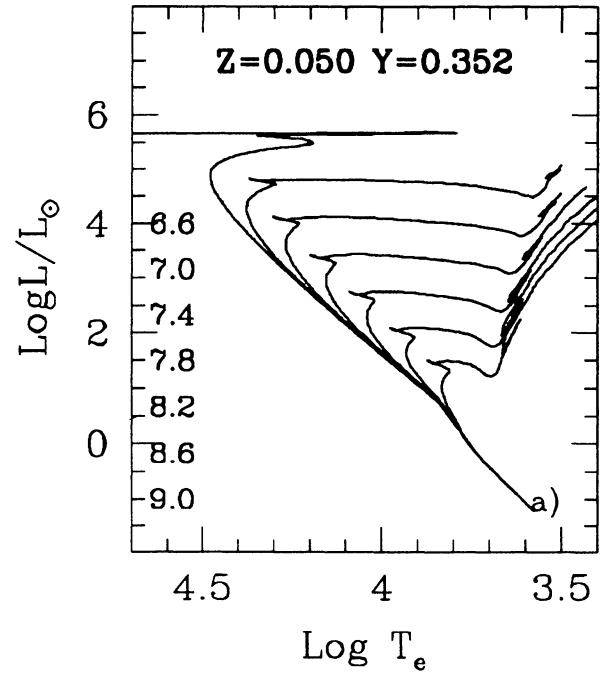
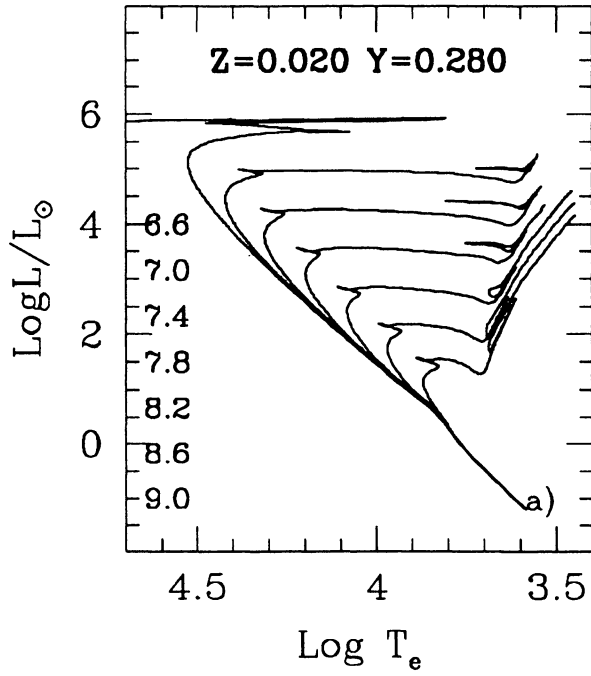


**Fig. 5.** The same as in Fig. 1, but for the composition  $[Z=0.020, Y=0.280]$

**Fig. 6.** The same as in Fig. 1, but for the composition  $[Z=0.050, Y=0.352]$



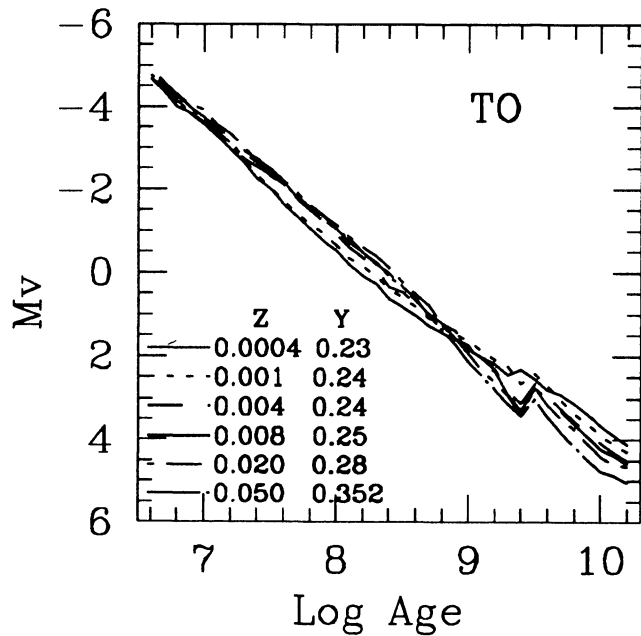


**Fig. 7.** The absolute visual magnitude  $M_V$  of the turn-off (TO) as function of the age (logarithmic value in years) and the chemical composition as indicated

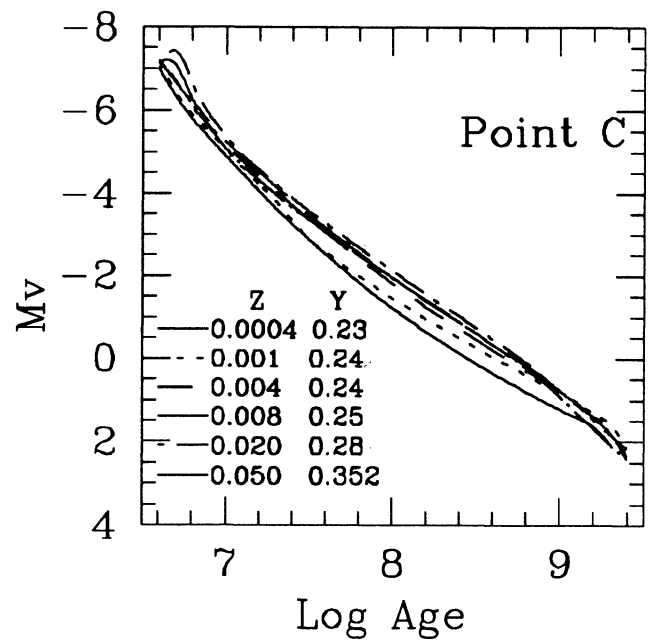


**Fig. 9.** The absolute visual magnitude  $M_V$  of central exhaustion stage of core H-burning (stage C) as function of the age (logarithmic value in years) and the chemical composition as indicated

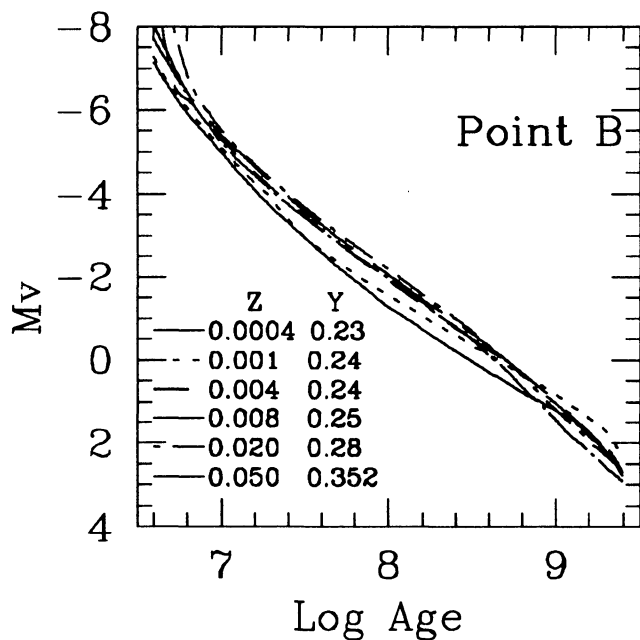


**Fig. 8.** The absolute visual magnitude  $M_V$  of the coolest stage of core H-burning (stage B) as function of the age (logarithmic value in years) and the chemical composition as indicated

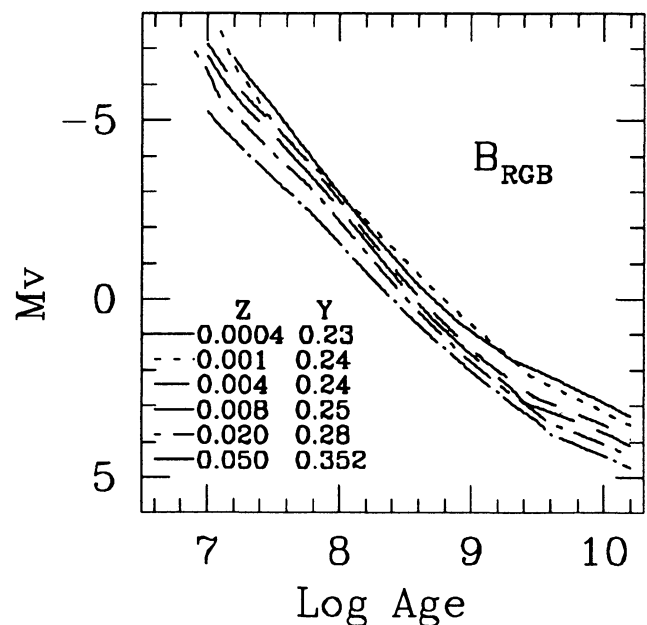


**Fig. 10.** The absolute visual magnitude  $M_V$  of the stage at the bottom of the RGB ( $B_{\text{RGB}}$ ) as function of the age (logarithmic value in years) and the chemical composition as indicated

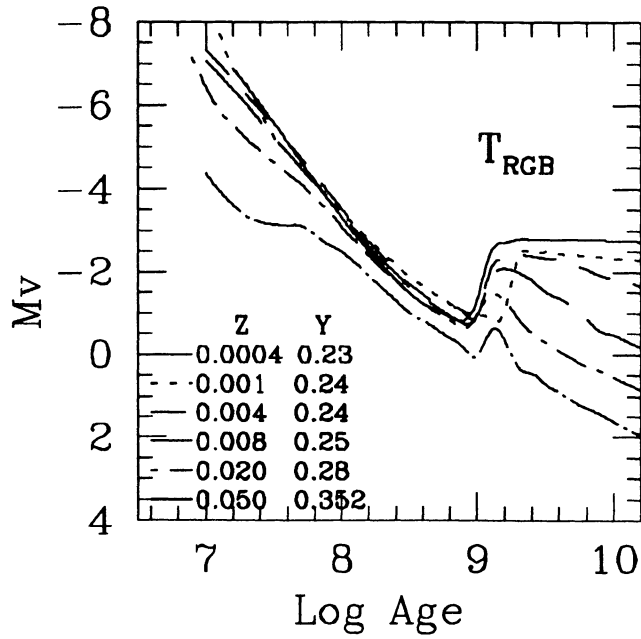


**Fig. 11.** The absolute visual magnitude  $M_V$  of the tip of the RGB ( $T_{\text{RGB}}$ ) as function of the age (logarithmic value in years) and the chemical composition as indicated

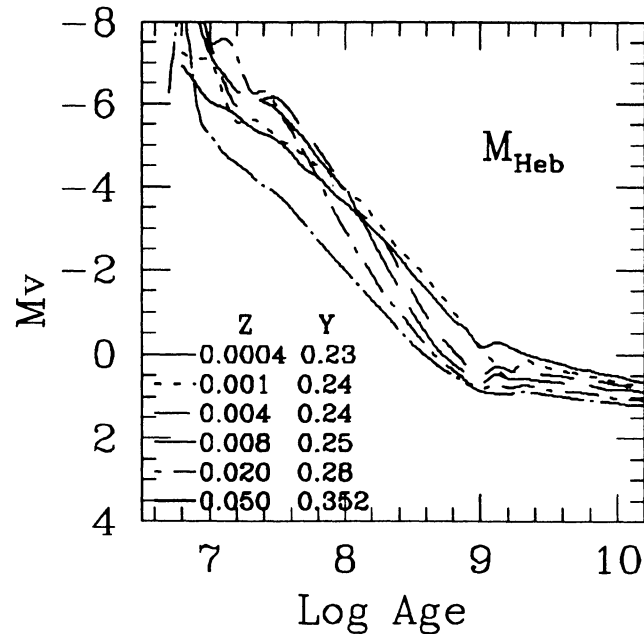


**Fig. 12.** The absolute visual magnitude  $M_V$  of the mean locus of stationary core He-burning ( $M_{\text{HeB}}$ ) as function of the age (logarithmic value in years) and the chemical composition as indicated

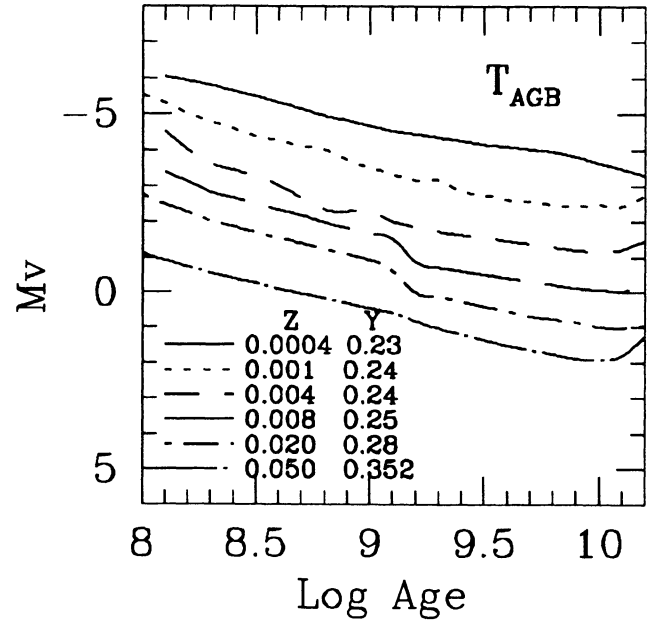


**Fig. 13.** The absolute visual magnitude  $M_V$  of the tip of the AGB ( $T_{\text{AGB}}$ ) as function of the age (logarithmic value in years) and the chemical composition as indicated

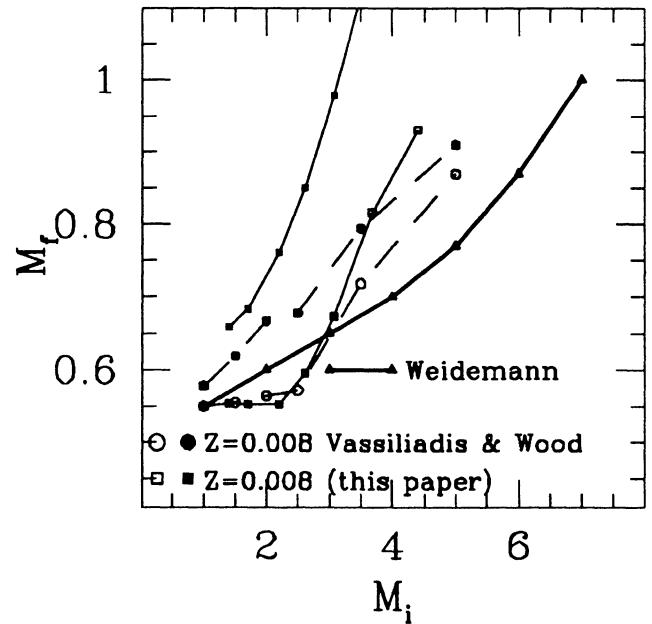


**Fig. 14.** The  $M_f(M_i)$  relationship. The solid line is the empirical relation by Weidemann (1987). Open circles and squares show the relation between the core mass at the start of the TP-AGB phase and the initial mass of the star according to the models by Vassiliadis & Wood (1993) and the present models, respectively. Filled symbols show the  $M_f(M_i)$  relation. The meaning of the symbols is the same as before. The masses are in solar units. See the text for more detail about the model structure and efficiency of mass loss. The theoretical relationships are for the typical composition [ $Z=0.008$ ,  $Y=0.250$ ]

Table 7.

 $Z = 0.0004 \quad Y = 0.230$ 

Age	Phase	M	$T_{eff}$	L	$M_V$	B-V	V-I	V-J	V-K
10.2	TO	0.772	3.809	0.307	4.110	0.406	0.578	0.879	1.169
	BRGB	0.788	3.751	0.658	3.289	0.584	0.763	1.209	1.627
	TRGB	0.794	3.637	3.271	-2.743	1.292	1.327	2.160	2.916
	MHeb	0.667	3.848	1.649	0.654	0.231	0.357	0.589	0.763
	TAGB	0.668	3.573	-3.282	1.418	1.507	2.434	3.268	
10.1	TO	0.818	3.819	0.390	3.891	0.379	0.542	0.820	1.083
	BRGB	0.838	3.752	0.733	3.098	0.579	0.758	1.203	1.618
	TRGB	0.845	3.640	3.268	-2.759	1.269	1.309	2.129	2.875
	MHeb	0.730	3.771	1.715	0.593	0.496	0.680	1.076	1.439
	TAGB	0.732	3.610	3.689	-3.476	1.448	1.353	2.551	3.427
10.0	TO	0.868	3.891	0.477	3.662	0.348	0.496	0.751	0.980
	BRGB	0.890	3.753	0.808	2.909	0.574	0.783	1.196	1.606
	TRGB	0.898	3.643	3.258	-2.764	1.240	1.287	2.089	2.823
	MHeb	0.795	3.753	1.762	0.508	0.557	0.747	1.184	1.591
	TAGB	0.797	3.604	3.779	-3.636	1.465	1.327	2.628	3.538
9.9	TO	0.922	3.846	0.585	3.382	0.314	0.442	0.667	0.867
	BRGB	0.947	3.756	0.879	2.728	0.565	0.745	1.184	1.587
	TRGB	0.957	3.646	3.255	-2.783	1.215	1.266	2.054	2.777
	MHeb	0.863	3.746	1.788	0.459	0.588	0.778	1.234	1.660
	TAGB	0.866	3.599	3.867	-3.817	1.475	1.357	2.675	3.610
9.8	TO	0.978	3.865	0.678	3.138	0.271	0.376	0.556	0.717
	BRGB	1.005	3.758	0.950	2.547	0.556	0.737	1.170	1.567
	TRGB	1.018	3.649	3.247	-2.789	1.189	1.246	2.019	2.730
	MHeb	0.934	3.743	1.821	0.382	0.597	0.787	1.248	1.680
	TAGB	0.938	3.596	3.927	-3.946	1.480	1.373	2.697	3.646
9.7	TO	1.038	3.886	0.766	2.907	0.213	0.281	0.422	0.542
	BRGB	1.071	3.758	1.024	2.360	0.555	0.736	1.168	1.565
	TRGB	1.085	3.651	3.245	-2.797	1.175	1.234	2.001	2.706
	MHeb	1.009	3.741	1.841	0.336	0.606	0.766	1.264	1.701
	TAGB	1.015	3.596	3.959	-4.021	1.481	1.376	2.702	3.654
9.6	TO	1.094	3.910	0.813	2.795	0.152	0.233	0.360	0.460
	BRGB	1.142	3.756	1.097	2.183	0.563	0.745	1.182	1.587
	TRGB	1.158	3.652	3.240	-2.799	1.159	1.221	1.981	2.680
	MHeb	1.091	3.741	1.883	0.231	0.605	0.795	1.262	1.689
	TAGB	1.097	3.595	3.988	-4.092	1.482	1.378	2.704	3.657
9.5	TO	1.168	3.934	0.924	2.545	0.096	0.160	0.202	0.262
	BRGB	1.217	3.752	1.167	2.014	0.576	0.759	1.204	1.620
	TRGB	1.237	3.654	3.233	-2.797	1.139	1.206	1.958	2.650
	MHeb	1.179	3.742	1.915	0.149	0.601	0.791	1.255	1.689
	TAGB	1.187	3.596	4.010	-4.155	1.480	1.371	2.695	3.643
9.4	TO	1.249	3.959	1.039	2.323	0.048	0.040	0.062	0.080
	BRGB	1.299	3.751	1.236	1.843	0.578	0.763	1.210	1.628
	TRGB	1.323	3.657	3.226	-2.796	1.115	1.188	1.931	2.615
	MHeb	1.273	3.744	1.948	0.062	0.595	0.785	1.245	1.676
	TAGB	1.285	3.596	4.050	-4.253	1.480	1.373	2.698	3.647
9.3	TO	1.333	3.955	0.991	2.433	0.058	0.051	0.079	0.098
	BRGB	1.384	3.754	1.079	2.207	0.055	0.051	0.081	0.101
	TRGB	1.408	3.658	3.233	-2.795	1.115	1.188	1.931	2.615
	MHeb	1.331	3.749	1.901	0.081	0.584	0.770	1.220	1.643
	TAGB	1.342	3.661	3.215	-2.795	1.080	1.162	1.891	2.563
9.2	TO	1.400	3.977	1.092	2.052	0.584	0.774	1.227	1.651
	BRGB	1.453	3.751	1.183	1.843	0.057	0.050	0.081	0.101
	TRGB	1.478	3.668	3.236	-2.796	1.115	1.188	1.931	2.615
	MHeb	1.384	3.747	1.992	0.052	0.584	0.774	1.227	1.651
	TAGB	1.400	3.597	4.083	-4.345	1.478	1.367	2.688	3.641
9.1	TO	1.499	4.005	1.233	2.019	-0.015	-0.024	-0.061	-0.082
	BRGB	1.552	3.751	1.246	-0.197	0.567	0.757	1.200	1.614
	TRGB	1.581	3.669	3.165	-2.715	1.020	1.119	1.819	2.468
	MHeb	1.512	3.751	1.411	1.407	0.584	0.771	1.222	1.646
	TAGB	1.531	3.599	4.117	-4.440	1.476	1.358	2.676	3.612
9.0	TO	1.597	4.033	1.433	1.432	-0.054	-0.052	-0.120	-0.153
	BRGB	1.621	3.749	1.508	1.164	0.581	0.769	1.218	1.641
	TRGB	1.651	3.668	3.171	-2.712	1.020	1.133	1.831	2.485
	MHeb	1.581	3.751	1.411	1.407	0.584	0.771	1.222	1.646
	TAGB	1.607	3.597	4.083	-4.345	1.478	1.367	2.688	3.641

 $Z = 0.0004 \quad Y = 0.230$



Table 7. continued

 $Z = 0.0004$ 
 $\bar{Y} = 0.230$ 
 $Z = 0.0004$ 
 $Y = 0.230$ 

Age	Phase	M	$T_{eff}$	L	$\dot{M}_V$	B-V	V-I	V-J	V-K
8.2	RHeb	3.501	3.722	2.806	-2.040	0.681	0.862	1.386	1.871
	MHeb	3.574	3.917	2.979	-2.666	0.016	0.092	0.180	0.232
	BHeb	3.619	3.980	3.045	-2.611	-0.055	0.002	-0.006	-0.006
	TAGB	3.687	3.609	4.623	-5.798	1.451	1.591	2.566	3.448
	TO	3.400	4.212	2.479	-0.073	-0.157	-0.163	-0.376	-0.492
8.1	B	3.795	4.193	2.761	-0.746	-0.153	-0.152	-0.348	-0.460
	C	3.824	4.237	2.834	-0.663	-0.171	-0.173	-0.409	-0.532
	RHeb	3.837	3.729	2.806	-2.055	0.651	0.836	1.340	1.808
	TAGB	3.839	3.710	3.010	-2.511	0.749	0.919	1.477	1.999
	TO	3.874	3.719	2.972	-2.446	0.700	0.878	1.410	1.904
8.0	RHeb	3.944	3.947	3.141	-2.984	-0.029	0.041	0.077	0.093
	MHeb	4.000	4.012	3.219	-2.890	-0.076	-0.018	-0.070	-0.093
	TAGB	4.068	3.615	4.650	-5.925	1.435	1.551	2.496	3.346
	TO	3.840	4.237	2.649	-0.200	-0.168	-0.175	-0.409	-0.532
	B	4.243	4.219	2.930	-1.015	-0.166	-0.165	-0.382	-0.502
7.9	B	4.283	4.262	3.002	-0.939	-0.182	-0.187	-0.439	-0.572
	C	4.299	3.726	2.983	-2.493	0.665	0.848	1.359	1.834
	RHeb	4.301	3.707	3.172	-2.906	0.767	0.934	1.500	2.030
	MHeb	4.339	3.715	3.144	-2.865	0.721	0.896	1.436	1.941
	TAGB	4.427	3.969	3.302	-3.305	-0.050	0.016	0.024	0.024
7.8	B	4.498	4.035	3.375	-3.163	-0.087	-0.033	-0.107	-0.144
	C	4.568	3.621	4.671	-6.039	1.418	1.506	2.420	3.236
	RHeb	4.300	4.263	2.836	-0.519	-0.180	-0.190	-0.440	-0.574
	TAGB	4.750	4.244	3.091	-1.267	-0.177	-0.176	-0.417	-0.543
	TO	4.807	4.288	3.174	-1.222	-0.194	-0.204	-0.468	-0.612
7.7	B	4.821	3.724	3.164	-2.942	0.674	0.856	1.371	1.850
	C	4.823	3.703	3.341	-3.316	0.787	0.951	1.527	2.065
	RHeb	4.851	3.711	3.320	-3.291	0.743	0.915	1.464	1.980
	MHeb	4.932	3.991	3.466	-3.613	-0.062	-0.004	-0.025	-0.036
	TAGB	4.997	4.058	3.531	-3.439	-0.098	-0.044	-0.144	-0.189
7.6	B	5.066	3.650	4.411	-5.671	1.251	1.292	2.063	2.762
	C	5.383	4.270	3.284	-1.604	-0.188	-0.191	-0.448	-0.585
	RHeb	4.800	4.289	2.993	-0.760	-0.194	-0.204	-0.469	-0.613
	TAGB	5.435	4.313	3.355	-1.521	-0.206	-0.216	-0.492	-0.648
	TO	5.450	3.719	3.361	-3.420	0.701	0.881	1.406	1.898
7.5	B	5.452	3.700	3.521	-3.756	0.810	0.969	1.556	2.102
	C	5.482	3.707	3.506	-3.742	0.769	0.936	1.498	2.024
	RHeb	5.585	4.027	3.647	-3.886	-0.083	-0.025	-0.091	-0.124
	MHeb	5.658	4.080	3.701	-3.744	-0.105	-0.061	-0.181	-0.237
	TAGB	5.720	3.660	4.357	-5.624	1.155	1.214	1.941	2.602
7.4	B	6.084	4.296	3.471	-1.062	-0.207	-0.217	-0.497	-0.651
	C	6.144	4.339	3.542	-1.841	-0.219	-0.228	-0.526	-0.686
	RHeb	6.160	3.713	3.564	-3.905	0.740	0.912	1.456	1.967
	TAGB	6.898	4.320	3.658	-2.241	-0.212	-0.216	-0.498	-0.657
	TO	6.953	4.364	3.727	-2.169	-0.232	-0.240	-0.552	-0.723
7.3	B	6.967	3.706	3.758	-4.372	0.779	0.942	1.507	2.032
	C	6.968	3.693	3.895	-4.657	0.866	1.007	1.620	2.185
	RHeb	6.379	4.100	3.869	-4.049	-0.116	-0.076	-0.210	-0.280
	MHeb	6.448	3.666	4.362	-5.677	1.100	1.172	1.878	2.517
	TAGB	6.150	4.342	3.352	-1.345	-0.220	-0.230	-0.530	-0.690
7.2	B	6.898	4.320	3.658	-2.241	-0.212	-0.216	-0.498	-0.657
	C	6.953	4.364	3.727	-2.169	-0.232	-0.240	-0.552	-0.723
	RHeb	6.967	3.706	3.758	-4.372	0.779	0.942	1.507	2.032
	TAGB	6.968	3.693	3.895	-4.657	0.866	1.007	1.620	2.185
	TO	6.995	3.699	3.884	-4.662	0.823	0.976	1.565	2.106
7.1	B	7.146	4.092	4.005	-4.435	-0.109	-0.067	-0.195	-0.260
	C	7.216	4.119	4.036	-4.363	-0.123	-0.087	-0.240	-0.313
	RHeb	7.305	3.669	4.424	-5.847	1.084	1.160	1.858	2.490
	MHeb	7.350	4.368	3.526	-1.635	-0.230	-0.243	-0.557	-0.730
	TAGB	6.950	4.368	3.526	-1.635	-0.230	-0.243	-0.557	-0.730
7.0	B	7.934	4.344	3.852	-2.592	-0.225	-0.231	-0.532	-0.693
	C	8.002	4.388	3.921	-2.513	-0.244	-0.253	-0.579	-0.725
	RHeb	8.017	3.704	3.955	-4.856	0.797	0.955	1.528	2.043
	TAGB	8.019	3.688	4.092	-5.129	0.905	1.033	1.663	2.243
	TO	8.052	3.695	4.076	-5.124	0.853	0.996	1.599	2.152
6.9	B	8.177	4.100	4.176	-4.814	-0.112	-0.072	-0.206	-0.276
	C								
	RHeb								
	TAGB								
	TO								

Table 8. continued

Z = 0.001 Y = 0.230

Age	Phase	M	$T_{eff}$	L	$M_V$	B-V	V-I	V-J	V-K
9.1	BRGB	1.573	3.737	1.437	1.353	0.652	0.811	1.283	1.731
	TRGB	1.584	3.672	1.472	1.013	0.981	1.070	1.767	2.412
	MHeb	1.620	3.731	1.767	0.538	0.673	0.828	1.322	1.785
	TAGB	1.669	3.537	1.466	-3.159	1.564	2.564	3.913	5.084
	TO	1.563	3.989	1.269	1.845	-0.004	-0.014	-0.029	-0.039
9.0	B	1.688	3.956	1.514	1.109	0.031	0.035	0.062	0.070
	C	1.698	4.005	1.615	1.061	-0.034	-0.035	-0.070	-0.093
	BRGB	1.705	3.734	1.570	1.026	0.663	0.820	1.300	1.755
	TRGB	1.714	3.680	2.406	-0.888	0.937	1.031	1.699	2.317
	MHeb	1.761	3.737	1.899	0.194	0.645	0.804	1.279	1.726
8.9	TAGB	1.818	3.538	4.112	-3.315	1.564	3.866	5.032	6.538
	TO	1.692	4.012	1.406	1.615	-0.029	-0.041	-0.083	-0.108
	B	1.846	3.979	1.660	0.821	-0.007	-0.001	-0.011	-0.012
	C	1.856	4.030	1.756	0.835	-0.059	-0.055	-0.118	-0.153
	BRGB	1.863	3.731	1.703	0.698	0.673	0.828	1.320	1.781
8.8	TRGB	1.869	3.683	2.423	-0.946	0.918	1.016	1.674	2.281
	MHeb	1.917	3.745	2.020	-0.127	0.612	0.774	1.229	1.654
	TAGB	1.972	3.539	4.176	-3.507	1.563	5.250	3.833	4.966
	TO	1.825	4.035	1.511	1.473	-0.053	-0.057	-0.128	-0.166
	B	2.005	4.001	1.799	0.581	-0.036	-0.031	-0.063	-0.084
8.7	C	2.019	4.054	1.895	0.612	-0.076	-0.067	-0.139	-0.206
	BRGB	2.026	3.729	1.837	0.367	0.682	0.836	1.337	1.805
	TRGB	2.032	3.685	2.460	-1.046	0.907	1.008	1.658	2.258
	MHeb	2.096	3.768	2.179	-0.571	0.522	0.692	1.090	1.456
	TAGB	2.157	3.540	4.236	-3.705	1.562	2.491	3.779	4.936
8.6	TO	1.981	4.059	1.646	1.258	-0.073	-0.074	-0.167	-0.220
	B	2.201	4.025	1.932	0.372	-0.058	-0.050	-0.108	-0.141
	C	2.220	4.077	2.035	0.390	-0.098	-0.088	-0.196	-0.255
	BRGB	2.226	3.728	1.979	0.013	0.685	0.839	1.343	1.813
	TRGB	2.231	3.685	2.532	-1.225	0.910	1.010	1.661	2.262
8.5	MHeb	2.294	3.805	2.334	-1.020	0.397	0.553	0.857	1.129
	TAGB	2.348	3.549	4.241	-3.999	1.556	2.290	3.477	4.602
	TO	2.158	4.082	1.767	1.085	-0.091	-0.092	-0.205	-0.267
	B	2.408	4.049	2.087	0.108	-0.077	-0.062	-0.150	-0.196
	C	2.421	4.101	2.177	0.168	-0.110	-0.102	-0.235	-0.299
8.4	BRGB	2.427	3.727	2.121	-0.340	0.688	0.841	1.349	1.821
	TRGB	2.431	3.684	2.614	-1.426	0.917	1.015	1.669	2.272
	MHeb	2.458	3.715	2.288	-0.729	0.748	0.890	1.437	1.941
	TAGB	2.503	3.848	2.519	-1.544	0.227	0.342	0.559	0.803
	TO	2.552	3.542	4.354	-4.090	1.561	2.438	3.680	4.828
8.3	B	2.661	4.106	1.917	0.841	-0.102	-0.105	-0.240	-0.313
	C	2.684	4.073	2.232	-0.123	-0.097	-0.082	-0.189	-0.247
	BRGB	2.658	4.125	2.321	-0.056	-0.117	-0.113	-0.264	-0.347
	TRGB	2.665	3.724	2.268	-0.701	0.701	0.853	1.370	1.848
	MHeb	2.669	3.682	2.709	-1.656	0.929	1.025	1.684	2.292
8.2	TAGB	2.707	3.709	2.458	-1.136	0.780	0.913	1.481	2.003
	TO	2.743	3.843	2.622	-1.800	0.362	0.588	0.771	0.912
	B	2.766	3.875	2.677	-1.957	0.133	0.227	0.391	0.512
	C	2.804	3.543	4.408	-4.248	1.561	2.425	3.656	4.800
	BRGB	2.600	4.129	2.072	0.591	-0.115	-0.117	-0.272	-0.356
8.1	TRGB	2.902	4.098	2.381	-0.355	-0.110	-0.098	-0.229	-0.293
	MHeb	2.919	4.150	2.466	-0.273	-0.133	-0.122	-0.295	-0.387
	TAGB	2.925	3.720	2.417	-1.067	0.723	0.870	1.399	1.885
	TO	2.929	3.681	2.805	-1.888	0.940	1.034	1.697	2.310
	B	2.968	3.702	2.630	-1.544	0.815	0.939	1.528	2.069
8.0	C	3.007	3.841	2.778	-2.193	0.241	0.366	0.596	0.782
	BRGB	3.033	3.598	2.827	-2.326	0.063	0.149	0.263	0.340
	TRGB	3.079	3.542	4.477	-4.370	1.561	2.454	3.710	4.860
	MHeb	2.850	4.153	2.209	-0.390	-0.129	-0.129	-0.304	-0.398
	TO	3.222	4.124	2.534	-0.594	-0.119	-0.111	-0.262	-0.344
7.9	B	3.245	4.175	2.617	-0.499	-0.149	-0.139	-0.328	-0.437
	C	3.253	3.714	2.573	-1.442	0.753	0.891	1.440	1.942
	BRGB	3.257	3.677	2.929	-2.184	0.961	1.051	1.724	2.346
	TRGB	3.308	3.697	2.788	-1.922	0.844	0.960	1.566	2.121
	MHeb								

Table 7. continued

Z = 0.0004 Y = 0.230

Age	Phase	M	$T_{eff}$	L	$M_V$	B-V	V-I	V-J	V-K
6.6	LM	45.953	3.728	5.797	-9.567	0.696	0.849	1.343	1.776
	TO	32.000	4.626	5.312	-4.664	-0.310	-0.319	-0.729	-0.969
	B	57.000	4.466	5.919	-7.157	-0.280	-0.280	-0.663	-0.883
	C	57.562	4.511	5.953	-6.992	-0.290	-0.300	-0.700	-0.924
Table 8.									
$Z = 0.001 \quad Y = 0.230$									
Age	Phase	M	$T_{eff}$	L	$M_V$	B-V	V-I	V-J	V-K
10.2	TO	0.776	3.796	0.229	4.301	0.456	0.616	0.946	1.267
	BRGB	0.797	3.741	0.565	3.524	0.638	0.795	1.261	1.696
	TRGB	0.805	3.306	3.306	-2.297	1.519	1.739	2.803	3.834
	MHeb	0.634	3.870	1.608	0.735	0.181	0.267	0.445	0.575
	TAGB	0.636	3.587	3.469	-2.754	1.521	1.692	2.743	3.743
10.1	TO	0.822	3.805	0.314	4.080	0.427	0.582	0.891	1.189
	BRGB	0.848	3.749	0.623	3.368	0.610	0.768	1.214	1.633
	TRGB	0.857	3.583	3.303	-2.316	1.512	1.713	2.771	3.790
	MHeb	0.703	3.743	1.689	0.702	0.617	0.779	1.240	1.671
	TAGB	0.705	3.552	3.593	-2.450	1.554	2.231	3.404	4.521
10.0	TO	0.869	3.816	0.388	3.886	0.397	0.545	0.828	1.099
	BRGB	0.899	3.751	0.699	3.175	0.603	0.762	1.204	1.618
	TRGB	0.911	3.586	3.300	-2.338	1.502	1.684	2.734	3.741
	MHeb	0.773	3.722	1.728	0.653	0.712	0.862	1.386	1.870
	TAGB	0.776	3.543	3.700	-2.480	1.561	2.424	3.654	4.798
9.9	TO	0.923	3.829	0.494	3.612	0.364	0.504	0.754	0.988
	BRGB	0.958	3.745	0.785	2.970	0.623	0.782	1.239	1.666
	TRGB	0.971	3.590	3.297	-2.369	1.489	1.644	2.684	3.674
	MHeb	0.848	3.720	1.768	0.559	0.719	0.868	1.397	1.884
	TAGB	0.851	3.537	3.787	-2.446	1.565	2.572	3.929	5.101
9.8	TO	0.982	3.846	0.591	3.359	0.322	0.441	0.659	0.861
	BRGB	1.019	3.748	0.852	2.798	0.612	0.772	1.222	1.642
	TRGB	1.035	3.594	3.291	-2.399	1.474	1.599	2.628	3.601
	MHeb	0.924	3.716	1.791	0.512	0.740	0.885	1.428	1.929
	TAGB	0.929	3.533	3.854	-2.480	1.567	2.651	4.076	5.263
9.7	TO	1.050	3.868	0.714	3.037	0.265	0.360	0.528	0.684
	BRGB	1.086	3.745	0.925	2.620	0.622	0.782	1.239	1.666
	TRGB	1.103	3.599	3.284	-2.428	1.457	1.550	2.568	3.524
	MHeb	1.004	3.716	1.821	0.437	0.741	0.885	1.429	1.931
	TAGB	1.010	3.533	3.896	-2.575	1.567	2.657	4.086	5.274
9.6	TO	1.123	3.893	0.838	2.715	0.195	0.242	0.371	0.477
	BRGB	1.159	3.745	0.997	2.440	0.623	0.783	1.239	1.668
	TRGB	1.180	3.602	3.281	-2.456	1.444	1.515	2.524	3.469
	MHeb	1.091	3.715	1.841	0.390	0.743	0.887	1.433	1.937
	TAGB	1.099	3.532	3.927	-2.630	1.567	2.670	4.111	5.301
9.5	TO	1.204	3.916	0.954	2.431	0.134	0.150	0.236	0.300
	BRGB	1.237	3.743	1.071	2.258	0.628	0.789	1.248	1.681
	TRGB	1.263	3.606	3.278	-2.494	1.424	1.481	2.471	3.394
	MHeb	1.184	3.717	1.869	0.317	0.736	0.882	1.423	1.923
	TAGB	1.193	3.533	3.960	-2.748	1.567	2.649	4.071	5.258
9.4	TO	1.288	3.912	0.865	2.657	0.151	0.170	0.261	0.332
	B	1.285	3.904	0.987	2.340	0.166	0.195	0.304	0.386
	C	1.293	3.940	1.081	2.149	0.079	0.082	0.128	0.160
	BRGB	1.334	3.740	1.173	2.009	0.640	0.800	1.266	1.706
	TRGB	1.365	3.614	3.236	-2.475	1.381	1.421	2.371	3.255
9.3	TO	1.307	3.719	1.903	0.226	0.726	0.875	1.409	1.902
	MHeb	1.325	3.534	3.994	-2.860	1.566	2.633	4.042	5.276
	TAGB	1.357	3.938	1.046	2.235	0.087	0.088	0.138	0.171
	TO	1.439	3.916	1.729	1.712	0.118	0.140	0.230	0.290
	C	1.446	3.965	1.343	1.569	0.025	0.023	0.035	0.037
9.2	BRGB	1.455	3.739	1.317	1.650	0.642	0.802	1.268	1.709
	TRGB	1.475	3.626	3.129	-2.339	1.301	1.327	2.218	3.037
	MHeb	1.487	3.734	1.922	0.166	0.702	0.854	1.372	1.853
	TAGB	1.507	3.541	3.992	-3.150	1.562	2.459	3.719	4.870
	TO	1.447	3.966	1.138	2.085	0.036	0.025	0.035	0.040
9.2	B	1.557	3.936	1.375	1.401	0.070	0.083	0.138	0.173
	C	1.565	3.983	1.472	1.315	-0.007	-0.009	-0.019	-0.024

Table 8. continued

Z = 0.001 Y = 0.230												
Age	Phase	M	T <sub>eff</sub>	L	M <sub>V</sub>	B-V	V-I	V-J	V-K			
8.3	M <sub>Heb</sub>	3.345	3.810	2.904	-2.470	0.361	0.512	0.804	1.061			
	B <sub>Heb</sub>	3.385	3.909	2.979	-2.693	0.030	0.112	0.204	0.264			
	T <sub>AGB</sub>	3.428	3.543	4.539	-4.577	1.561	2.424	3.654	4.799			
	T <sub>O</sub>	3.200	4.178	2.390	0.083	-0.142	-0.141	-0.337	-0.443			
	B	3.378	4.150	2.690	-0.830	-0.135	-0.123	-0.295	-0.388			
	C	3.601	4.200	2.770	-0.737	-0.159	-0.157	-0.365	-0.474			
	B <sub>RGB</sub>	3.609	3.708	2.732	-1.820	0.785	0.915	1.484	2.005			
	T <sub>RGB</sub>	3.611	3.674	3.057	-2.486	0.981	1.069	1.753	2.385			
	R <sub>Heb</sub>	3.658	3.693	2.945	-2.293	0.875	0.982	1.605	2.174			
	M <sub>Heb</sub>	3.696	3.837	3.061	-2.907	0.242	0.372	0.615	0.808			
8.2	B <sub>Heb</sub>	3.732	3.919	3.125	-3.035	0.005	0.083	0.158	0.205			
	T <sub>AGB</sub>	3.777	3.545	4.598	-4.785	1.559	2.382	3.589	4.726			
	T <sub>O</sub>	3.350	4.203	2.538	-0.141	-0.155	-0.159	-0.369	-0.482			
	C	3.934	4.176	2.846	-1.064	-0.150	-0.140	-0.330	-0.437			
	B	3.957	4.224	2.921	-0.968	-0.169	-0.168	-0.393	-0.518			
	B <sub>RGB</sub>	3.964	3.702	2.890	-2.196	0.819	0.941	1.531	2.069			
	T <sub>RGB</sub>	3.969	3.672	3.180	-2.780	0.998	1.083	1.776	2.416			
	R <sub>Heb</sub>	4.013	3.688	3.102	-2.663	0.905	1.007	1.643	2.227			
	M <sub>Heb</sub>	4.066	3.868	3.218	-3.326	0.124	0.236	0.409	0.535			
	B <sub>Heb</sub>	4.106	3.933	3.269	-3.361	-0.017	0.065	0.108	0.144			
8.1	T <sub>AGB</sub>	4.170	3.548	4.651	-4.996	1.557	2.315	3.507	4.636			
	T <sub>O</sub>	3.900	4.228	2.886	-0.358	-0.165	-0.169	-0.398	-0.526			
	B	4.391	4.202	3.004	-1.314	-0.162	-0.155	-0.367	-0.476			
	C	4.423	4.251	3.080	-1.215	-0.179	-0.178	-0.425	-0.555			
	B <sub>RGB</sub>	4.432	3.696	3.051	-2.575	0.855	0.967	1.577	2.132			
	T <sub>RGB</sub>	4.434	3.667	3.325	-3.117	1.031	1.105	1.818	2.473			
	R <sub>Heb</sub>	4.485	3.682	3.253	-3.018	0.941	1.035	1.689	2.290			
	M <sub>Heb</sub>	4.534	3.890	3.364	-3.685	0.062	0.158	0.291	0.374			
	B <sub>Heb</sub>	4.580	3.965	3.420	-3.624	-0.049	0.021	0.023	0.024			
	T <sub>AGB</sub>	4.637	3.566	4.606	-5.301	1.545	1.957	3.071	4.152			
8.0	T <sub>AGB</sub>	4.400	4.253	2.870	-0.672	-0.176	-0.182	-0.428	-0.561			
	T <sub>O</sub>	4.872	4.227	3.163	-1.559	-0.173	-0.169	-0.397	-0.521			
	C	4.904	4.276	3.238	-1.465	-0.197	-0.196	-0.456	-0.595			
	B <sub>RGB</sub>	4.912	3.690	3.212	-2.951	0.892	0.995	1.624	2.197			
	T <sub>RGB</sub>	4.914	3.663	3.464	-3.443	1.060	1.124	1.854	2.520			
	R <sub>Heb</sub>	4.958	3.677	3.405	-3.372	0.981	1.063	1.736	2.355			
	M <sub>Heb</sub>	5.023	3.953	3.529	-3.943	-0.039	0.033	0.052	0.066			
	B <sub>Heb</sub>	5.068	3.996	3.568	-3.853	-0.066	-0.006	-0.043	-0.059			
	T <sub>AGB</sub>	5.143	3.569	4.665	-5.509	1.544	1.905	3.008	4.082			
	T <sub>O</sub>	4.900	4.278	3.037	-0.945	-0.196	-0.199	-0.459	-0.598			
7.9	B	5.449	4.252	3.325	-1.818	-0.183	-0.179	-0.427	-0.556			
	C	5.489	4.300	3.399	-1.723	-0.210	-0.210	-0.479	-0.639			
	B <sub>RGB</sub>	5.500	3.685	3.373	-3.330	0.926	1.023	1.667	2.257			
	T <sub>RGB</sub>	5.502	3.658	3.617	-3.795	1.097	1.150	1.900	2.582			
	R <sub>Heb</sub>	5.550	3.672	3.563	-3.737	1.018	1.088	1.784	2.419			
	M <sub>Heb</sub>	5.615	3.962	3.672	-4.262	-0.044	0.030	0.032	0.036			
	B <sub>Heb</sub>	5.669	4.026	3.718	-4.078	-0.083	-0.023	-0.098	-0.130			
	T <sub>AGB</sub>	5.749	3.585	4.572	-5.488	1.528	1.715	2.771	3.781			
	T <sub>O</sub>	5.450	4.303	3.182	-1.163	-0.208	-0.211	-0.485	-0.642			
	B	6.075	4.277	3.487	-2.084	-0.199	-0.194	-0.457	-0.597			
7.8	C	6.127	4.325	3.561	-1.982	-0.220	-0.221	-0.513	-0.674			
	B <sub>RGB</sub>	6.138	3.680	3.535	-3.711	0.966	1.050	1.713	2.321			
	T <sub>RGB</sub>	6.141	3.653	3.771	-4.150	1.136	1.177	1.946	2.644			
	R <sub>Heb</sub>	6.194	3.666	3.721	-4.103	1.056	1.115	1.833	2.485			
	M <sub>Heb</sub>	6.274	3.995	3.827	-4.500	-0.062	0.003	-0.038	-0.050			
	B <sub>Heb</sub>	6.339	4.054	3.869	-4.309	-0.096	0.038	-0.139	-0.186			
	T <sub>AGB</sub>	6.404	3.617	4.309	-5.158	1.421	1.442	2.384	3.238			
	T <sub>O</sub>	6.100	4.328	3.352	-1.438	-0.218	-0.223	-0.516	-0.678			
	B	6.839	4.302	3.655	-2.359	-0.210	-0.210	-0.481	-0.641			
	C	6.890	4.349	3.727	-2.263	-0.226	-0.233	-0.537	-0.710			
7.7	B <sub>RGB</sub>	6.900	3.673	3.699	-4.086	1.013	1.083	1.773	2.402			
	T <sub>RGB</sub>	6.902	3.649	3.920	-4.488	1.175	1.207	1.994	2.709			
	R <sub>Heb</sub>	6.949	3.661	3.883	-4.473	1.098	1.144	1.884	2.554			
	M <sub>Heb</sub>	7.039	4.029	3.984	-4.725	-0.082	-0.020	-0.098	-0.132			
	B <sub>Heb</sub>	7.121	4.078	4.021	-4.560	-0.109	-0.059	-0.178	-0.237			
	T <sub>AGB</sub>	7.121	3.653	3.771	-4.150	1.136	1.177	1.946	2.644			
	R <sub>Heb</sub>	7.121	3.653	3.771	-4.150	1.136	1.177	1.946	2.644			
	M <sub>Heb</sub>	7.121	3.653	3.771	-4.150	1.136	1.177	1.946	2.644			
	B <sub>Heb</sub>	7.121	3.653	3.771	-4.150	1.136	1.177	1.946	2.644			
	T <sub>RGB</sub>	7.121	3.653	3.771	-4.150	1.136	1.177	1.946	2.644			
7.6	T <sub>AGB</sub>	7.209	3.619	4.391	-5.357	1.417	1.430	2.363	3.206			
	T <sub>O</sub>	7.650	4.353	3.514	-0.225	-0.541	-0.541	-0.716	-0.886			
	B	7.800	4.326	3.829	-2.647	-0.221	-0.222	-0.514	-0.677			
	C	7.871	4.373	3.902	-2.563	-0.237	-0.246	-0.563	-0.749			
	B <sub>RGB</sub>	7.884	3.668	3.874	-4.493	1.051	1.109	1.821	2.466			
	T <sub>RGB</sub>	7.884	3.644	4.087	-4.866	1.222	1.243	2.052	2.785			
	R <sub>Heb</sub>	7.943	3.656	4.053	-4.863	1.144	1.178	1.937	2.623			
	M <sub>Heb</sub>	8.048	4.058	4.147	-4.985	-0.098	-0.145	-0.213	-0.293			
	B <sub>Heb</sub>	8.123	4.100	4.178	-4.836	-0.112	-0.172	-0.214	-0.278			
	T <sub>RGB</sub>	8.216	3.613	4.549	-5.704	1.455	1.486	2.448	3.320			
7.5	T <sub>O</sub>	7.850	4.379	3.696	-2.007	-0.237	-0.249	-0.568	-0.756			
	B	8.822	4.351	4.008	-2.956	-0.230	-0.235	-0.539	-0.714			
	C	8.890	4.398	4.079	-2.873	-0.250	-0.257	-0.590	-0.780			
	B <sub>RGB</sub>	8.901	3.663	4.050	-4.902	1.092	1.137	1.868	2.529			
	T <sub>RGB</sub>	8.904	3.640	4.258	-5.250	1.270	1.279	2.112	2.864			
	R <sub>Heb</sub>	8.954	3.651	4.223	-5.251	1.192	1.214	1.994	2.698			
	M <sub>Heb</sub>	9.129	4.106	4.321	-5.161	-0.115	-0.175	-0.220	-0.290			
	B <sub>Heb</sub>	9.220	4.127	4.343	-5.096	-0.128	-0.186	-0.250	-0.334			
	T <sub>AGB</sub>	9.366	3.612	4.725	-6.119	1.476	1.509	2.478	3.353			
	T <sub>O</sub>	8.900	4.405	3.880	-2.329	-0.249	-0.264	-0.598	-0.792			
7.4	B	10.400	4.371	4.228	-3.398	-0.238	-0.245	-0.560	-0.746			
	C	10.517	4.417	4.306	-3.341	-0.255	-0.266	-0.613	-0.814			
	B <sub>RGB</sub>	10.533	3.673	4.253	-5.466	1.044	1.097	1.789	2.410			
	T <sub>RGB</sub>	10.536	3.651	4.478	-5.832	1.217	1.228	2.007	2.707			
	R <sub>Heb</sub>	10.632	3.662	4.428	-5.832	1.134	1.165	1.897	2.556			
	M <sub>Heb</sub>	10.772	4.131	4.510	-5.489	-0.129	-0.188	-0.255	-0.340			
	B <sub>Heb</sub>	10.871	4.170	4.533	-5.324	-0.149	-0.118	-0.314	-0.412			
	T <sub>AGB</sub>	11.011	3.633	4.866	-6.674	1.402	1.378	2.244	3.006			
	T <sub>O</sub>	10.500	4.432	4.091	-2.713	-0.260	-0.271	-0.631	-0.831			
	B	12.150	4.390	4.461	-3.883	-0.246	-0.251	-0.581	-0.771			
7.3	C	12.266	4.436	4.533	-3.823	-0.263	-0.273	-0.636	-0.844			
	B <sub>RGB</sub>	12.285	3.662	4.707	-6.029	0.988	1.054	1.705	2.289			
	T <sub>RGB</sub>	12.285	3.662	4.707	-6.029	0.988	1.054	1.705	2.289			
	R <sub>Heb</sub>	12.407	3.672	4.625	-6.383	1.078	1.121	1.812	2.431			
	M <sub>Heb</sub>	12.562	4.195	4.700	-5.802	-0.158	-0.129	-0.348	-0.455			
	B <sub>Heb</sub>	12.627	4.217	4.709	-5.498	-0.168	-0.144	-0.492	-0.602			
	T <sub>AGB</sub>	12.827	3.647	5.005	-7.134	1.319	1.300	2.101	2.803			
	T <sub>O</sub>	12.200	4.459	4.304	-3.114	-0.278	-0.288	-0.658	-0.876			
	B	14.222	4.408	4.653	-4.273	-0.256	-0.256	-0.602	-0.798			
	C	14.337	4.454	4.723	-4.218	-0.271	-0.281	-0.655	-0.869			
7.2	B <sub>RGB</sub>	14.353	3.686	4.655	-6.532	0.982	1.050	1.691	2.268			
	T <sub>RGB</sub>	14.355	3.662	4.855	-6.886	1.175	1.190	1.923	2.575			
	M <sub>Heb</sub>	14.509	4.272	4.859	-5.561	-0.193	-0.177	-0.447	-0.585			
	B <sub>Heb</sub>	14.609	4.272	4.859	-5.561	-0.193	-0.177	-0.447	-0.585			
	R <sub>Heb</sub>	14.881	3.673	4.785	-6.785	1.084	1.124	1.812	2.428			
	T <sub>AGB</sub>	14.891	3.653	5.094	-7.409	1.278	1.263	2.033	2.706			



Table 8. continued

 $Z = 0.001$   $Y = 0.230$ 

Age	Phase	M	$T_{eff}$	L	M <sub>V</sub>	B-V	V-I	V-J	V-K
6.8	TO	21.600	4.561	4.912	-4.124	-0.300	-0.306	-0.716	-0.952
	B	30.900	4.455	5.449	-6.039	-0.270	-0.280	-0.655	-0.871
	C	31.202	4.502	5.490	-5.899	-0.288	-0.296	-0.684	-0.924
6.7	M <sub>H</sub> eb	32.616	4.295	5.586	-7.253	-0.204	-0.192	-0.472	-0.626
	LM	34.216	4.052	5.610	-8.670	-0.096	-0.036	-0.137	-0.182
	TO	26.800	4.585	5.130	-4.509	-0.304	-0.310	-0.720	-0.960
	B	40.427	4.455	5.663	-6.575	-0.270	-0.280	-0.655	-0.871
6.6	M <sub>H</sub> eb	41.156	4.503	5.706	-6.435	-0.288	-0.297	-0.685	-0.925
	LM	46.544	3.785	5.753	-9.624	0.379	0.345	0.899	1.178
	TO	32.000	4.611	5.304	-4.768	-0.310	-0.313	-0.723	-0.963
	B	57.829	4.438	5.919	-7.289	-0.265	-0.275	-0.639	-0.849
	C	58.272	4.487	5.950	-7.160	-0.280	-0.283	-0.670	-0.897

Table 9.

 $Z = 0.004$   $Y = 0.240$ 

Age	Phase	M	$T_{eff}$	L	M <sub>V</sub>	B-V	V-I	V-J	V-K
10.2	TO	0.810	3.777	0.149	4.489	0.549	0.673	1.041	1.394
	BRGB	0.836	3.731	0.407	3.925	0.727	0.833	1.329	1.792
	TRGB	0.847	3.544	3.356	-1.656	1.590	2.403	3.615	4.755
	M <sub>H</sub> eb	0.674	3.719	1.670	0.788	0.776	0.875	1.407	1.890
10.1	TO	0.675	3.531	3.491	-1.484	1.594	2.703	4.172	5.368
	BRGB	0.856	3.786	0.224	4.290	0.517	0.644	0.991	1.324
	TRGB	0.887	3.734	0.482	3.730	0.714	0.821	1.306	1.759
	M <sub>H</sub> eb	0.899	3.549	3.355	-1.769	1.585	2.304	3.493	4.620
10.0	TO	0.743	3.701	1.709	0.751	0.869	0.954	1.542	2.084
	BRGB	0.746	3.516	3.626	-1.230	1.599	3.052	4.819	6.081
	TRGB	0.903	3.795	0.309	4.070	0.485	0.614	0.941	1.254
	M <sub>H</sub> eb	0.941	3.737	3.562	-3.522	0.703	0.811	1.287	1.731
9.9	TO	0.957	3.552	3.354	-1.834	1.582	2.248	3.425	4.544
	BRGB	0.813	3.696	1.732	0.715	0.890	0.973	1.578	2.136
	TRGB	0.817	3.506	3.720	-1.169	1.601	3.240	5.146	6.432
	M <sub>H</sub> eb	0.955	3.804	0.397	3.840	0.454	0.584	0.887	1.180
9.8	TO	0.998	3.734	0.622	3.380	0.714	0.821	1.304	1.757
	BRGB	1.016	3.555	3.353	-1.920	1.579	2.171	3.331	4.440
	TRGB	0.887	3.697	1.776	0.603	0.886	0.970	1.572	2.129
	M <sub>H</sub> eb	0.969	3.498	3.844	-1.291	1.601	3.372	5.362	6.656
9.7	TO	1.080	3.827	0.627	3.246	0.378	0.499	0.753	0.990
	BRGB	1.014	3.815	0.507	3.553	0.417	0.546	0.823	1.091
	TRGB	1.061	3.733	0.686	3.222	0.717	0.824	1.310	1.766
	M <sub>H</sub> eb	1.082	3.563	3.348	-2.075	1.571	2.028	3.158	4.248
9.6	TO	1.050	3.498	3.879	-1.380	1.601	3.370	5.359	6.653
	BRGB	1.149	3.842	0.743	2.948	0.339	0.452	0.670	0.870
	TRGB	1.194	3.730	0.809	2.923	0.730	0.835	1.330	1.795
	M <sub>H</sub> eb	1.223	3.572	3.347	-2.303	1.562	1.831	2.918	3.982
9.5	TO	1.127	3.568	3.348	-2.200	1.566	1.921	3.027	4.103
	BRGB	1.151	3.696	1.789	0.571	0.886	0.971	1.574	2.131
	TRGB	1.043	3.696	1.789	0.571	0.886	0.971	1.574	2.131
	M <sub>H</sub> eb	1.050	3.498	3.879	-1.380	1.601	3.370	5.359	6.653
9.4	TO	1.127	3.568	3.348	-2.200	1.566	1.921	3.027	4.103
	BRGB	1.151	3.696	1.789	0.571	0.886	0.971	1.574	2.131
	TRGB	1.043	3.696	1.789	0.571	0.886	0.971	1.574	2.131
	M <sub>H</sub> eb	1.050	3.498	3.879	-1.380	1.601	3.370	5.359	6.653
9.3	TO	1.127	3.568	3.348	-2.200	1.566	1.921	3.027	4.103
	BRGB	1.151	3.696	1.789	0.571	0.886	0.971	1.574	2.131
	TRGB	1.043	3.696	1.789	0.571	0.886	0.971	1.574	2.131
	M <sub>H</sub> eb	1.050	3.498	3.879	-1.380	1.601	3.370	5.359	6.653

Table 9. continued

 $Z = 0.004$   $Y = 0.240$ 

Age	Phase	M	$T_{eff}$	L	M <sub>V</sub>	B-V	V-I	V-J	V-K
9.2	TO	1.471	3.730	1.071	2.267	0.730	0.836	1.332	1.797
	BRGB	1.501	3.589	3.313	-2.410	1.511	1.638	2.682	3.679
	TRGB	1.841	3.703	1.841	0.416	0.851	0.943	1.522	2.059
	M <sub>H</sub> eb	1.469	3.501	3.996	-1.734	1.601	3.328	5.581	6.581
9.1	TO	1.422	3.896	0.981	2.325	0.191	0.221	0.339	0.433
	BRGB	1.562	3.858	1.223	1.723	0.279	0.371	0.555	0.719
	TRGB	1.575	3.918	1.360	1.388	0.108	0.129	0.208	0.264
	M <sub>H</sub> eb	1.615	3.732	1.176	1.998	0.721	0.829	1.318	1.777
9.0	TO	1.619	3.503	4.028	-1.861	1.601	3.295	5.526	6.526
	BRGB	1.524	3.918	1.099	2.048	0.128	0.139	0.215	0.274
	TRGB	1.589	3.879	1.361	1.359	0.215	0.270	0.422	0.541
	M <sub>H</sub> eb	1.712	3.730	1.289	1.721	0.728	0.836	1.331	1.794
8.9	TO	1.741	3.672	3.037	-2.068	1.330	1.356	2.262	3.109
	BRGB	1.821	3.712	1.872	0.308	0.805	0.903	1.454	1.962
	TRGB	1.910	3.500	4.112	-2.016	1.601	3.333	5.298	6.589
	M <sub>H</sub> eb	1.826	3.941	1.204	1.830	0.075	0.069	0.111	0.141
8.8	TO	1.844	3.903	1.515	0.979	0.139	0.169	0.274	0.354
	BRGB	1.859	3.964	1.637	0.808	0.014	0.014	0.025	0.030
	TRGB	1.870	3.731	1.422	1.382	0.721	0.830	1.320	1.778
	M <sub>H</sub> eb	1.888	3.665	2.458	-0.941	1.054	1.107	1.832	2.498
8.7	TO	1.990	3.720	1.778	0.519	0.769	0.869	1.399	1.884
	BRGB	2.094	3.504	4.176	-2.265	1.601	3.271	5.197	6.484
	TRGB	2.094	3.966	1.412	1.382	0.026	0.012	0.023	0.025
	M <sub>H</sub> eb	2.016	3.929	1.660	0.654	0.069	0.089	0.149	0.189
8.6	TO	2.038	3.989	1.789	0.537	-0.028	-0.020	-0.039	-0.052
	BRGB	2.049	3.728	1.561	1.043	0.735	0.842	1.344	1.811
	TRGB	2.063	3.671	2.479	-1.029	1.024	1.080	1.782	2.425
	M <sub>H</sub> eb	2.172	3.723	1.870	0.281	0.756	0.859	1.378	1.855
8.5	TO	2.286	3.501	4.220	-2.292	1.601	3.328	5.291	6.582
	BRGB	2.251	3.726	1.708	0.679	0.741	0.847	1.355	1.824
	TRGB	2.262	3.674	2.519	-1.147	1.011	1.067	1.760	2.393
	M <sub>H</sub> eb	2.379	3.726	2.018	-0.099	0.744	0.850	1.359	1.827
8.4	TO	2.143	4.019	1.664	0.991	-0.050	-0.048	-0.106	-0.136
	BRGB	2.424	3.980	1.978	0.023	-0.020	-0.011	-0.019	-0.025
	TRGB	2.444	4.038	2.086	0.031	-0.075	-0.064	-0.141	-0.182
	M <sub>H</sub> eb	2.453	3.725	1.856	0.313	0.747	0.852	1.365	1.837
8.3	TO	2.461	3.677	2.546	-1.235	0.995	1.052	1.733	2.352
	BRGB	2.585	3.731	2.148	-0.436	0.721	0.832	1.324	1.778
	TRGB	2.585	3.731	2.148	-0.436	0.721	0.832	1.324	1.778
	M <sub>H</sub> eb	2.629	3.740	2.327	-0.906	0.682	0.801	1.263	1.693
8.2	TO	2.736	3.504	4.333	-2.656	1.601	3.272	5.199	6.486
	BRGB	2.706	3.645	1.803	0.772	-0.069	-0.072	-0.156	-0.198
	TRGB	2.671	4.006	2.132	-0.241	-0.055	-0.036	-0.082	-0.105
	M <sub>H</sub> eb	2.695	3.723	2.018	-0.087	0.758	0.861	1.382	1.859
8.1	TO	2.705	3.723	2.018	-0.087	0.758	0.861	1.382	1.859
	BRGB	2.713	3.675	2.640	-1.457	1.007	1.062	1.750	2.377
	TRGB	2.729	3.740	2.327	-0.906	0.682	0.801	1.263	1.693
	M <sub>H</sub> eb	2.829	3.509	4.426	-3.003	1.600	3.192	5.069	6.352
8.0	TO	2.583	4.070	1.978	0.471	-0.091	-0.085	-0.196	-0.252
	BRGB	2.938	4.033	2.292	-0.506	-0.078	-0.058	-0.131	-0.171
	TRGB	2.963	4.089	2.400	-0.483	-0.109	-0.092	-0.220	-0.287
	M <sub>H</sub> eb	2.972	3.720	2.184	-0.499	0.771	0.871	1.401	1.883
7.9	TO	2.978	3.672	2.746	-1.704	1.026	1.077	1.777	2.414
	BRGB	3.114	3.758	2.529	-1.461	0.598	0.734	1.142	1.524
	TRGB	3.242	3.512	4.494	-3.231	1.600	3.153	5.004	6.284
	M <sub>H</sub> eb	2.790	4.097	2.084	0.348	-0.105	-0.100	-0.232	-0.302
7.8	TO	2.987	4.061	2.469	-0.802	-0.097	-0.074	-0.180	-0.231
	BRGB	3.287	4.116	2.565	-0.740	-0.125	-0.107	-0.259	-0.340
	TRGB	3.312	3.715	2.366	-0.937	0.798	0.895	1.439	1.937
	M <sub>H</sub> eb	3.323	3.715	2.366	-0.937	0.798	0.895	1.439	1.937

Table 9. continued

 $Z = 0.004$ 
 $Y = 0.240$ 

Age	Phase	M	$T_{eff}$	L	$M_V$	B-V	V-I	V-J	V-K
8.3	RHeb	3.378	3.707	2.487	-1.215	0.839	0.927	1.494	2.014
	BHeb	3.405	3.799	2.649	-1.827	0.437	0.575	0.878	1.160
	RHeb	3.465	3.797	2.737	-2.047	0.443	0.582	0.890	1.175
	TAGB	3.569	3.513	4.553	-3.441	1.600	3.116	4.937	6.211
	TO	3.216	4.124	3.225	-2.099	-0.121	-0.116	-0.272	-0.355
	B	3.650	4.090	2.640	-1.080	-0.113	-0.089	-0.219	-0.288
	C	3.674	4.144	2.732	-1.002	-0.133	-0.124	-0.297	-0.386
	TRGB	3.683	3.709	2.549	-1.377	0.830	0.919	1.481	1.995
	TRGB	3.689	3.664	3.044	-2.401	1.083	1.121	1.851	2.519
	RHeb	3.744	3.701	2.702	-1.730	0.880	0.954	1.547	2.084
8.2	BHeb	3.775	3.843	2.886	-2.492	0.243	0.346	0.571	0.754
	TRGB	3.816	3.837	2.945	-2.636	0.259	0.370	0.609	0.803
	TAGB	3.897	3.513	4.622	-3.606	1.600	3.120	4.944	6.218
	TO	3.587	4.151	2.492	-0.359	-0.132	-0.132	-0.308	-0.401
	B	4.017	4.118	2.811	-1.344	-0.128	-0.106	-0.259	-0.341
	C	4.050	4.171	2.899	-1.258	-0.151	-0.138	-0.333	-0.436
	TRGB	4.060	3.704	2.734	-1.820	0.863	0.942	1.524	2.052
	TRGB	4.065	3.660	3.187	-2.737	1.108	1.139	1.882	2.561
	RHeb	4.148	3.693	2.915	-2.231	0.921	0.985	1.603	2.160
	BHeb	4.197	3.887	3.113	-3.065	0.093	0.176	0.310	0.395
8.1	TRGB	4.227	3.875	3.142	-3.147	0.120	0.215	0.375	0.483
	TAGB	4.317	3.520	4.669	-4.000	1.597	2.957	4.842	5.886
	TO	3.958	4.179	2.660	-0.612	-0.150	-0.143	-0.344	-0.454
	B	4.508	4.146	2.987	-1.626	-0.137	-0.123	-0.300	-0.390
	C	4.543	4.198	3.074	-1.537	-0.163	-0.152	-0.367	-0.480
	TRGB	4.552	3.699	2.929	-2.291	0.895	0.963	1.563	2.102
	TRGB	4.556	3.655	3.361	-3.141	1.146	1.165	1.931	2.626
	RHeb	4.638	3.686	3.122	-2.714	0.969	1.022	1.668	2.251
	BHeb	4.666	3.814	3.258	-3.392	0.342	0.472	0.750	0.999
	TRGB	4.688	3.917	3.211	-3.525	0.015	0.088	0.165	0.204
8.0	TRGB	4.780	3.531	4.703	-4.511	1.594	2.704	4.174	5.371
	TAGB	4.749	4.207	2.849	-0.916	-0.162	-0.161	-0.383	-0.495
	TO	5.007	4.174	3.169	-1.914	-0.156	-0.139	-0.337	-0.439
	B	5.046	4.226	3.252	-1.814	-0.178	-0.168	-0.404	-0.524
	C	5.056	3.693	3.124	-2.755	0.927	0.988	1.604	2.159
	TRGB	5.061	3.550	3.532	-3.529	1.183	1.194	1.983	2.694
	RHeb	5.164	3.678	3.328	-3.192	1.018	1.058	1.735	2.342
	BHeb	5.207	3.869	3.472	-3.978	0.120	0.229	0.398	0.515
	TRGB	5.239	3.853	3.517	-3.924	-0.039	0.025	0.044	0.055
	LM	5.301	3.578	4.416	-5.050	1.554	1.762	2.831	3.871
7.9	TO	5.000	4.235	3.032	-1.211	-0.182	-0.174	-0.416	-0.538
	B	5.646	4.202	3.355	-2.218	-0.167	-0.151	-0.369	-0.486
	C	5.684	4.253	3.436	-2.115	-0.189	-0.183	-0.438	-0.568
	TRGB	5.692	3.686	3.316	-3.202	0.971	1.022	1.665	2.243
	TRGB	5.696	3.642	3.721	-3.941	1.237	1.241	2.063	2.804
	RHeb	5.793	3.578	3.528	-3.648	1.069	1.097	1.800	2.432
	BHeb	5.828	3.858	3.653	-4.431	0.147	0.267	0.453	0.597
	TRGB	5.867	3.966	3.705	-4.338	-0.050	0.018	0.014	0.014
	LM	5.909	3.597	4.328	-5.010	1.513	1.585	2.611	3.568
	TO	5.650	4.264	3.213	-1.493	-0.194	-0.193	-0.451	-0.585
7.8	B	6.342	4.229	3.540	-2.515	-0.180	-0.169	-0.409	-0.529
	C	6.387	4.280	3.620	-2.418	-0.201	-0.171	-0.471	-0.612
	TRGB	6.396	3.680	3.505	-3.645	1.011	1.051	1.716	2.313
	TRGB	6.400	3.637	3.896	-4.335	1.286	1.280	2.123	2.887
	RHeb	6.511	3.663	3.723	-4.085	1.122	1.137	1.872	2.530
	BHeb	6.553	3.872	3.840	-4.903	0.094	0.209	0.371	0.479
	TRGB	6.591	3.948	3.877	-4.837	-0.035	0.041	0.063	0.078
	LM	6.635	3.601	4.366	-5.146	1.502	1.544	2.561	3.500
	TO	6.850	4.292	3.390	-1.770	-0.206	-0.206	-0.482	-0.628
	B	7.143	4.255	3.722	-2.825	-0.190	-0.181	-0.440	-0.570
7.7	C	7.200	4.306	3.802	-2.728	-0.213	-0.213	-0.498	-0.655
	TRGB	7.210	3.675	3.687	-4.073	1.048	1.078	1.760	2.372
	TRGB	7.215	3.632	4.077	-4.747	1.333	1.317	2.180	2.966
	RHeb	7.355	3.656	3.912	-4.515	1.172	1.171	1.938	2.617
	LM	7.402	3.858	4.014	-5.341	0.129	0.256	0.440	0.577
	TO	6.850	4.292	3.390	-1.770	-0.206	-0.206	-0.482	-0.628
	B	7.143	4.255	3.722	-2.825	-0.190	-0.181	-0.440	-0.570
	C	7.200	4.306	3.802	-2.728	-0.213	-0.213	-0.498	-0.655
	TRGB	7.210	3.675	3.687	-4.073	1.048	1.078	1.760	2.372
	TRGB	7.215	3.632	4.077	-4.747	1.333	1.317	2.180	2.966
7.6	RHeb	7.355	3.656	3.912	-4.515	1.172	1.171	1.938	2.617
	LM	7.402	3.858	4.014	-5.341	0.129	0.256	0.440	0.577
	TO	6.850	4.292	3.390	-1.770	-0.206	-0.206	-0.482	-0.628
	B	7.143	4.255	3.722	-2.825	-0.190	-0.181	-0.440	-0.570
	C	7.200	4.306	3.802	-2.728	-0.213	-0.213	-0.498	-0.655
	TRGB	7.210	3.675	3.687	-4.073	1.048	1.078	1.760	2.372
	TRGB	7.215	3.632	4.077	-4.747	1.333	1.317	2.180	2.966
	RHeb	7.355	3.656	3.912	-4.515	1.172	1.171	1.938	2.617
	LM	7.402	3.858	4.014	-5.341	0.129	0.256	0.440	0.577
	TO	6.850	4.292	3.390	-1.770	-0.206	-0.206	-0.482	-0.628
7.5	B	7.143	4.255	3.722	-2.825	-0.190	-0.181	-0.440	-0.570
	C	7.200	4.306	3.802	-2.728	-0.213	-0.213	-0.498	-0.655
	TRGB	7.210	3.675	3.687	-4.073	1.048	1.078	1.760	2.372
	TRGB	7.215	3.632	4.077	-4.747	1.333	1.317	2.180	2.966
	RHeb	7.355	3.656	3.912	-4.515	1.172	1.171	1.938	2.617
	LM	7.402	3.858	4.014	-5.341	0.129	0.256	0.440	0.577
	TO	6.850	4.292	3.390	-1.770	-0.206	-0.206	-0.482	-0.628
	B	7.143	4.255	3.722	-2.825	-0.190	-0.181	-0.440	-0.570
	C	7.200	4.306	3.802	-2.728	-0.213	-0.213	-0.498	-0.655
	TRGB	7.210	3.675	3.687	-4.073	1.048	1.078	1.760	2.372
7.4	TRGB	7.215	3.632	4.077	-4.747	1.333	1.317	2.180	2.966
	RHeb	7.355	3.656	3.912	-4.515	1.172	1.171	1.938	2.617
	LM	7.402	3.858	4.014	-5.341	0.129	0.256	0.440	0.577
	TO	6.850	4.292	3.390	-1.770	-0.206	-0.206	-0.482	-0.628
	B	7.143	4.255	3.722	-2.825	-0.190	-0.181	-0.440	-0.570
	C	7.200	4.306	3.802	-2.728	-0.213	-0.213	-0.498	-0.655
	TRGB	7.210	3.675	3.687	-4.073	1.048	1.078	1.760	2.372
	TRGB	7.215	3.632	4.077	-4.747	1.333	1.317	2.180	2.966
	RHeb	7.355	3.656	3.912	-4.515	1.172	1.171	1.938	2.617
	LM	7.402	3.858	4.014	-5.341	0.129	0.256	0.440	0.577
7.3	TO	6.850	4.292	3.390	-1.770	-0.206	-0.206	-0.482	-0.628
	B	7.143	4.255	3.722	-2.825	-0.190	-0.181	-0.440	-0.570
	C	7.200	4.306	3.802	-2.728	-0.213	-0.213	-0.498	-0.655
	TRGB	7.210	3.675	3.687	-4.073	1.048	1.078	1.760	2.372
	TRGB	7.215	3.632	4.077	-4.747	1.333	1.317	2.180	2.966
	RHeb	7.355	3.656	3.912	-4.515	1.172	1.171	1.938	2.617
	LM	7.402	3.858	4.014	-5.341	0.129	0.256	0.440	0.577
	TO	6.850	4.292	3.390	-1.770	-0.206	-0.206	-0.482	-0.628
	B	7.143	4.255	3.722	-2.825	-0.190	-0.181	-0.440	-0.570
	C	7.200	4.306	3.802	-2.728	-0.213	-0.213	-0.498	-0.655
7.2	TRGB	7.210	3.675	3.687	-4.073	1.048	1.078	1.760	2.372
	TRGB	7.215	3.632	4.077	-4.747	1.333	1.317	2.180	2.966
	RHeb	7.355	3.656	3.912	-4.515	1.172	1.171	1.938	2.617
	LM	7.402	3.858	4.014	-5.341	0.129	0.256	0.440	0.577
	TO	6.850	4.292	3.390	-1.770	-0.206	-0.206	-0.482	-0.628
	B	7.143	4.255	3.722	-2.825	-0.190	-0.181	-0.440	-0.570
	C	7.200	4.306	3.802	-2.728	-0.213	-0.213	-0.498	-0.655
	TRGB	7.210	3.675	3.687	-4.073	1.048	1.078	1.760	2.372
	TRGB	7.215	3.632	4.077	-4.747	1.333	1.317	2.180	2.966

Table 9. continued  
 $Z = 0.004$   $Y = 0.240$

Age	Phase	M	$T_{eff}$	L	$M_V$	B-V	V-I	V-J	V-K
6.9	TO	18.000	4.504	4.727	-3.991	-0.290	-0.309	-0.699	-0.939
	B	24.600	4.404	5.211	-5.759	-0.247	-0.254	-0.601	-0.799
	C	24.863	4.454	5.268	-5.629	-0.270	-0.285	-0.655	-0.879
	$R_{Heb}$	24.913	3.818	5.331	-8.626	0.259	0.404	0.667	0.869
	$B_{Heb}$	25.168	4.119	5.345	-7.668	-0.128	-0.080	-0.245	-0.325
	$H_{Heb}$	25.713	3.961	5.358	-8.477	-0.034	0.046	0.036	0.044
	$LM_{Heb}$	26.541	3.649	5.485	-8.374	1.341	1.271	2.058	2.744
6.8	TO	21.000	4.430	4.891	-4.262	-0.290	-0.310	-0.710	-0.949
	B	30.000	4.408	5.413	-6.258	-0.247	-0.252	-0.603	-0.802
	C	30.370	4.458	5.460	-6.087	-0.270	-0.288	-0.658	-0.885
	$M_{Heb}$	31.753	4.068	5.549	-8.466	-0.104	-0.054	-0.171	-0.225
	$R_{Heb}$	32.361	3.870	5.526	-9.116	0.243	0.393	0.649	0.845
	$B_{Heb}$	32.915	4.187	5.549	-7.802	-0.154	-0.128	-0.345	-0.449
	$LM_{Heb}$	33.618	3.818	5.615	-9.427	0.069	0.176	0.300	0.392
6.7	TO	25.800	4.556	5.082	-4.591	-0.304	-0.314	-0.718	-0.958
	B	39.723	4.391	5.636	-6.902	-0.240	-0.246	-0.582	-0.778
	C	39.994	4.440	5.676	-6.711	-0.265	-0.275	-0.645	-0.856
	$LM$	46.349	4.581	5.765	-6.133	-0.310	-0.320	-0.730	-0.970
6.6	TO	31.000	4.581	5.274	-4.907	-0.310	-0.320	-0.730	-0.970
	B	36.300	3.948	5.854	-9.762	-0.010	0.070	0.076	0.096
	C	37.449	4.477	5.909	-7.124	-0.280	-0.290	-0.670	-0.900
	$LM$	69.871	5.145	5.922	-2.596	-0.379	-0.392	-0.857	-1.143

Table 10.  
 $Z = 0.008$   $Y = 0.250$

Age	Phase	M	$T_{eff}$	L	$M_V$	B-V	V-I	V-J	V-K
10.2	TO	0.847	3.762	0.107	4.589	0.627	0.723	1.128	1.508
	$R_{Heb}$	0.878	3.714	0.351	4.107	0.817	0.894	1.452	1.965
	$B_{Heb}$	0.889	3.501	3.368	-0.178	1.612	3.318	5.274	6.565
	$H_{Heb}$	0.692	3.693	1.662	0.902	0.945	0.977	1.611	2.174
10.1	$T_{AGB}$	0.694	3.482	3.516	-0.100	1.615	3.627	5.779	7.088
	TO	0.894	3.771	0.193	4.366	0.591	0.690	1.072	1.429
	$R_{Heb}$	0.930	3.722	0.415	3.915	0.784	0.861	1.390	1.873
	$B_{Heb}$	0.945	3.506	3.376	-0.313	1.611	3.238	5.144	6.429
	$H_{Heb}$	0.770	3.689	1.694	0.838	0.962	0.983	1.642	2.219
	$T_{AGB}$	0.771	3.465	3.641	-0.043	1.618	3.865	6.198	7.524
10.0	TO	0.998	3.781	0.244	4.228	0.556	0.656	1.015	1.349
	$R_{Heb}$	0.985	3.725	0.484	3.735	0.772	0.849	1.369	1.843
	$B_{Heb}$	1.003	3.513	3.375	-0.471	1.609	3.130	4.964	6.240
	$H_{Heb}$	0.844	3.680	1.709	0.843	1.002	1.030	1.713	2.322
9.9	$T_{AGB}$	0.848	3.455	3.745	-0.064	1.620	4.050	6.468	7.804
	TO	0.996	3.790	0.366	3.911	0.519	0.622	0.936	1.268
	$R_{Heb}$	1.044	3.724	0.540	3.598	0.778	0.854	1.377	1.855
	$B_{Heb}$	1.067	3.517	3.361	-0.607	1.607	3.030	4.777	6.035
	$H_{Heb}$	0.923	3.680	1.723	0.808	1.002	1.030	1.715	2.324
9.8	$T_{AGB}$	0.928	3.449	3.816	-0.119	1.621	4.135	6.607	7.948
	TO	1.059	3.799	0.480	3.617	0.491	0.595	0.908	1.202
	$R_{Heb}$	1.110	3.722	0.602	3.449	0.786	0.861	1.389	1.872
	$B_{Heb}$	1.136	3.523	3.373	-0.867	1.603	2.894	4.526	5.758
	$H_{Heb}$	1.008	3.685	1.746	0.728	0.979	1.009	1.675	2.267
9.7	$T_{AGB}$	1.012	3.450	3.845	-0.217	1.621	4.117	6.578	7.918
	TO	1.129	3.810	0.601	3.303	0.453	0.560	0.848	1.110
	$R_{Heb}$	1.177	3.720	0.663	3.301	0.794	0.868	1.400	1.888
	$B_{Heb}$	1.205	3.530	3.373	-1.160	1.599	2.720	4.204	5.484
	$H_{Heb}$	1.089	3.685	1.759	0.697	0.979	1.010	1.677	2.270
9.6	$T_{AGB}$	1.094	3.452	3.873	-0.316	1.621	4.097	6.544	7.884
	TO	1.199	3.820	0.714	3.010	0.419	0.524	0.787	1.025
	$R_{Heb}$	1.242	3.721	0.717	3.164	0.794	0.867	1.397	1.865
	$B_{Heb}$	1.273	3.536	3.369	-1.366	1.595	2.593	3.967	5.143
	$H_{Heb}$	1.167	3.685	1.771	0.666	0.978	1.010	1.677	2.270
9.5	$T_{AGB}$	1.174	3.454	3.895	-0.417	1.620	4.065	6.492	7.829
	TO	1.265	3.831	0.816	2.749	0.382	0.481	0.716	0.932
	$R_{Heb}$	1.308	3.722	0.769	3.031	0.789	0.862	1.389	1.874
	$B_{Heb}$	1.352	3.540	3.370	-1.529	1.593	2.498	3.791	4.949
	$H_{Heb}$	1.267	3.686	1.783	0.633	0.972	1.005	1.668	2.266
9.4	$T_{AGB}$	1.219	3.455	3.922	-0.510	1.620	4.047	6.463	7.799
	TO	1.357	3.822	0.833	2.872	0.371	0.463	0.691	0.874

Table 10. continued  
 $Z = 0.008$   $Y = 0.250$

Age	Phase	M	$T_{eff}$	L	$M_V$	B-V	V-I	V-J	V-K
9.3	$T_{RGB}$	1.456	3.550	3.357	-1.802	1.584	2.281	3.466	4.590
	$M_{Heb}$	1.376	3.687	1.792	0.603	0.963	0.997	1.654	2.236
	$T_{AGB}$	1.395	3.457	3.942	-0.612	1.620	4.011	6.404	7.738
	TO	1.345	3.840	0.767	2.869	0.359	0.452	0.670	0.871
	C	1.508	3.813	1.046	2.181	0.436	0.546	0.826	1.077
9.2	$T_{RGB}$	1.517	3.858	1.193	1.777	0.293	0.364	0.550	0.712
	$M_{Heb}$	1.529	3.721	0.990	2.481	0.793	0.864	1.390	1.875
	$T_{AGB}$	1.562	3.562	3.322	-2.001	1.572	2.034	3.165	4.256
	$M_{Heb}$	1.498	3.689	1.802	0.568	0.953	0.989	1.638	2.214
	$T_{AGB}$	1.527	3.458	3.975	-2.079	1.620	4.001	6.388	7.722
9.1	TO	1.480	3.859	0.958	2.377	0.303	0.383	0.555	0.717
	C	1.629	3.825	1.181	1.829	0.396	0.499	0.749	0.972
	$T_{RGB}$	1.642	3.880	1.328	1.426	0.220	0.265	0.409	0.525
	$M_{Heb}$	1.655	3.724	1.103	2.189	0.784	0.856	1.375	1.855
	$T_{AGB}$	1.691	3.575	3.241	-2.084	1.558	1.787	2.865	3.920
9.0	$M_{Heb}$	1.651	3.694	1.778	0.610	0.930	0.971	1.603	2.164
	TO	1.714	3.460	4.017	-0.866	1.619	3.966	6.330	7.661
	C	1.883	3.883	1.009	2.237	0.228	0.272	0.408	0.522
	$T_{AGB}$	1.781	3.844	1.340	1.418	0.337	0.428	0.634	0.826
	TO	1.794	3.905	1.481	1.045	0.141	0.164	0.261	0.334
8.9	C	1.804	3.724	1.234	1.860	0.784	0.856	1.375	1.855
	$T_{RGB}$	1.833	3.598	3.046	-1.837	1.491	1.530	2.558	3.531
	$M_{Heb}$	1.918	3.700	1.819	0.478	0.898	0.945	1.551	2.090
	$T_{AGB}$	2.014	3.478	4.119	-1.517	1.616	3.690	5.881	7.195
	TO	1.720	3.910	1.215	1.725	0.146	0.155	0.244	0.314
8.8	C	1.930	3.867	1.480	1.046	0.253	0.310	0.482	0.622
	TO	1.815	3.937	1.293	1.578	0.080	0.077	0.125	0.159
	C	2.105	3.892	1.620	0.689	0.169	0.204	0.322	0.416
	$T_{RGB}$	2.129	3.953	1.764	0.439	0.022	0.027	0.048	0.068
	$T_{RGB}$	2.139	3.722	1.491	1.220	0.793	0.864	1.389	1.875
8.8	$T_{RGB}$	2.154	3.657	2.404	-0.755	1.127	1.144	1.916	2.611
	$M_{Heb}$	2.272	3.709	1.806	0.477	0.854	0.912	1.484	2.001
	$T_{AGB}$	2.400	3.478	4.232	-1.818	1.616	3.678	5.861	7.174
	TO	2.001	3.960	1.468	1.205	0.029	0.022	0.037	0.046
	C	2.306	3.918	1.781	0.307	0.087	0.111	0.187	0.238
8.7	C	2.325	3.979	1.912	0.163	-0.021	-0.010	-0.021	-0.027
	$T_{RGB}$	2.345	3.720	1.632	0.871	0.801	0.871	1.402	1.892
	$T_{RGB}$	2.345	3.656	2.480	-0.942	1.133	1.147	1.922	2.618
	$M_{Heb}$	2.469	3.711	1.909	0.213	0.848	0.960	1.471	1.981
	$T_{AGB}$	2.609	3.480	4.288	-1.982	1.616	3.660	5.832	7.144
8.6	$T_{AGB}$	2.179	3.986	1.597	0.983	-0.013	-0.017	-0.040	-0.047
	TO	2.400	4.011	1.769	0.673	-0.048	-0.041	-0.085	-0.107
	C	2.499	3.944	1.928	-0.001	0.033	0.048	0.085	0.107
	C	2.528	4.004	2.061	-0.094	-0.054	-0.034	-0.078	-0.101
	$T_{RGB}$	2.538	3.718	1.776	0.516	0.810	0.877	1.413	1.906
8.5	$T_{RGB}$	2.550	3.656	2.559	-1.139	1.138	1.150	1.925	2.621
	$M_{Heb}$	2.683	3.713	2.016	-0.063	0.841	0.898	1.455	1.959
	$T_{AGB}$	2.834	3.484	4.328	-2.182	1.615	3.592	5.720	7.028
	TO	2.400	4.011	1.769	0.673	-0.048	-0.041	-0.097	-0.122
	C	2.765	3.972	2.101	-0.332	-0.019	-0.004	-0.004	-0.008
8.5	C	2.786	4.031	2.220	-0.356	-0.078	-0.057	-0.132	-0.175
	$T_{RGB}$	2.795	3.718	1.939	0.110	0.813	0.877	1.413	1.904
	$T_{RGB}$	2.804	3.654	2.664	-1.389	1.153	1.160	1.942	2.644
	$M_{Heb}$	2.939	3.715	2.188	-0.500	0.835	0.891	1.441	1.937
	$T_{AGB}$	3.079	3.482	4.403	-2.326	1.615	3.623	5.772	7.081
8.5	TO	2.651	4.038	1.938	0.380	-0.076	-0.067	-0.145	-0.192
	C	3.037	4.000	2.269	-0.631	-0.056	-0.030	-0.070	-0.091
	C	3.060	4.058	2.379	-0.612	-0.094	-0.073	-0.176	-0.235
	$T_{RGB}$	3.071	3.717	2.105	-0.302	0.820	0.880	1.420	1.911
	$M_{Heb}$	3.080	3.653	2.767	-1.641	1.165	1.168	1.954	2.661
		3.227	3.724	2.361	-0.967	0.794	0.855	1.373	1.840

Table 10. continued

Z = 0.008 Y = 0.250

Age	Phase	M	$T_{eff}$	L	$M_V$	B-V	V-I	V-J	V-K
8.4	T <sub>AGB</sub>	3.381	3.484	4.458	-2.500	1.615	3.596	5.727	7.035
	TO	2.969	4.065	2.141	0.017	-0.093	-0.082	-0.187	-0.249
	B	3.385	4.029	2.440	-0.916	-0.081	-0.055	-0.127	-0.170
	C	3.408	4.086	2.546	-0.885	-0.110	-0.088	-0.220	-0.292
	BRGB	3.417	3.713	2.285	-0.738	0.843	0.896	1.452	1.952
	TRGB	3.425	3.648	2.911	-1.968	1.193	1.195	1.998	2.724
	M <sub>Heb</sub>	3.557	3.736	2.583	-1.562	0.737	0.804	1.285	1.712
	T <sub>Heb</sub>	3.683	3.484	4.520	-2.662	1.615	3.593	5.722	7.029
	TO	3.288	4.093	2.290	-0.205	-0.108	-0.098	-0.234	-0.304
	B	3.733	4.058	2.611	-1.193	-0.097	-0.070	-0.176	-0.234
8.3	C	3.756	4.115	2.714	-1.140	-0.126	-0.105	-0.261	-0.342
	BRGB	3.764	3.709	2.466	-1.176	0.868	0.912	1.485	1.995
	TRGB	3.770	3.644	3.053	-2.290	1.221	1.221	2.041	2.784
	M <sub>Heb</sub>	3.878	3.749	2.790	-2.116	0.677	0.757	1.195	1.588
	T <sub>AGB</sub>	3.985	3.484	4.583	-2.825	1.615	3.589	5.715	7.023
	TO	3.687	4.122	2.464	-0.477	-0.125	-0.114	-0.272	-0.354
	B	4.107	4.087	2.781	-1.469	-0.113	-0.086	-0.219	-0.293
	C	4.142	4.143	2.884	-1.406	-0.139	-0.122	-0.300	-0.395
	BRGB	4.151	3.703	2.651	-1.621	0.901	0.933	1.526	2.052
	TRGB	4.157	3.639	3.200	-2.620	1.255	1.247	2.091	2.853
8.2	M <sub>Heb</sub>	4.217	3.686	2.783	-1.875	0.989	1.008	1.664	2.250
	TRGB	4.244	3.786	2.956	-2.599	0.505	0.611	0.953	1.293
	B	4.304	3.781	3.017	-2.745	0.526	0.629	0.982	1.293
	C	4.142	4.087	2.884	-1.406	-0.139	-0.122	-0.300	-0.395
	BRGB	4.151	3.703	2.651	-1.621	0.901	0.933	1.526	2.052
	TRGB	4.157	3.639	3.200	-2.620	1.255	1.247	2.091	2.853
	M <sub>Heb</sub>	4.217	3.686	2.783	-1.875	0.989	1.008	1.664	2.250
	TRGB	4.244	3.786	2.956	-2.599	0.505	0.611	0.953	1.293
	B	4.304	3.781	3.017	-2.745	0.526	0.629	0.982	1.293
	C	4.142	4.087	2.884	-1.406	-0.139	-0.122	-0.300	-0.395
8.1	BRGB	4.151	3.703	2.651	-1.621	0.901	0.933	1.526	2.052
	TRGB	4.157	3.639	3.200	-2.620	1.255	1.247	2.091	2.853
	M <sub>Heb</sub>	4.217	3.686	2.783	-1.875	0.989	1.008	1.664	2.250
	TRGB	4.244	3.786	2.956	-2.599	0.505	0.611	0.953	1.293
	B	4.304	3.781	3.017	-2.745	0.526	0.629	0.982	1.293
	C	4.142	4.087	2.884	-1.406	-0.139	-0.122	-0.300	-0.395
	BRGB	4.151	3.703	2.651	-1.621	0.901	0.933	1.526	2.052
	TRGB	4.157	3.639	3.200	-2.620	1.255	1.247	2.091	2.853
	M <sub>Heb</sub>	4.217	3.686	2.783	-1.875	0.989	1.008	1.664	2.250
	TRGB	4.244	3.786	2.956	-2.599	0.505	0.611	0.953	1.293
8.0	B	4.304	3.781	3.017	-2.745	0.526	0.629	0.982	1.293
	C	4.142	4.087	2.884	-1.406	-0.139	-0.122	-0.300	-0.395
	BRGB	4.151	3.703	2.651	-1.621	0.901	0.933	1.526	2.052
	TRGB	4.157	3.639	3.200	-2.620	1.255	1.247	2.091	2.853
	M <sub>Heb</sub>	4.217	3.686	2.783	-1.875	0.989	1.008	1.664	2.250
	TRGB	4.244	3.786	2.956	-2.599	0.505	0.611	0.953	1.293
	B	4.304	3.781	3.017	-2.745	0.526	0.629	0.982	1.293
	C	4.142	4.087	2.884	-1.406	-0.139	-0.122	-0.300	-0.395
	BRGB	4.151	3.703	2.651	-1.621	0.901	0.933	1.526	2.052
	TRGB	4.157	3.639	3.200	-2.620	1.255	1.247	2.091	2.853
7.9	M <sub>Heb</sub>	4.217	3.686	2.783	-1.875	0.989	1.008	1.664	2.250
	TRGB	4.244	3.786	2.956	-2.599	0.505	0.611	0.953	1.293
	B	4.304	3.781	3.017	-2.745	0.526	0.629	0.982	1.293
	C	4.142	4.087	2.884	-1.406	-0.139	-0.122	-0.300	-0.395
	BRGB	4.151	3.703	2.651	-1.621	0.901	0.933	1.526	2.052
	TRGB	4.157	3.639	3.200	-2.620	1.255	1.247	2.091	2.853
	M <sub>Heb</sub>	4.217	3.686	2.783	-1.875	0.989	1.008	1.664	2.250
	TRGB	4.244	3.786	2.956	-2.599	0.505	0.611	0.953	1.293
	B	4.304	3.781	3.017	-2.745	0.526	0.629	0.982	1.293
	C	4.142	4.087	2.884	-1.406	-0.139	-0.122	-0.300	-0.395
7.8	BRGB	4.151	3.703	2.651	-1.621	0.901	0.933	1.526	2.052
	TRGB	4.157	3.639	3.200	-2.620	1.255	1.247	2.091	2.853
	M <sub>Heb</sub>	4.217	3.686	2.783	-1.875	0.989	1.008	1.664	2.250
	TRGB	4.244	3.786	2.956	-2.599	0.505	0.611	0.953	1.293
	B	4.304	3.781	3.017	-2.745	0.526	0.629	0.982	1.293
	C	4.142	4.087	2.884	-1.406	-0.139	-0.122	-0.300	-0.395
	BRGB	4.151	3.703	2.651	-1.621	0.901	0.933	1.526	2.052
	TRGB	4.157	3.639	3.200	-2.620	1.255	1.247	2.091	2.853
	M <sub>Heb</sub>	4.217	3.686	2.783	-1.875	0.989	1.008	1.664	2.250
	TRGB	4.244	3.786	2.956	-2.599	0.505	0.611	0.953	1.293
7.7	B	4.304	3.781	3.017	-2.745	0.526	0.629	0.982	1.293
	C	4.142	4.087	2.884	-1.406	-0.139	-0.122	-0.300	-0.395
	BRGB	4.151	3.703	2.651	-1.621	0.901	0.933	1.526	2.052
	TRGB	4.157	3.639	3.200	-2.620	1.255	1.247	2.091	2.853
	M <sub>Heb</sub>	4.217	3.686	2.783	-1.875	0.989	1.008	1.664	2.250
	TRGB	4.244	3.786	2.956	-2.599	0.505	0.611	0.953	1.293
	B	4.304	3.781	3.017	-2.745	0.526	0.629	0.982	1.293
	C	4.142	4.087	2.884	-1.406	-0.139	-0.122	-0.300	-0.395
	BRGB	4.151	3.703	2.651	-1.621	0.901	0.933	1.526	2.052
	TRGB	4.157	3.639	3.200	-2.620	1.255	1.247	2.091	2.853



Table 11. continued

 $Z = 0.02 \quad Y = 0.280$ 

Age	Phase	M	$T_{\text{eff}}$	L	$M_V$	B-V	V-I	V-J	V-K
9.4	TO	1.291	3.805	0.551	3.404	0.502	0.579	0.870	1.140
	B	1.489	3.784	0.861	2.649	0.575	0.646	0.988	1.298
	C	1.503	3.812	1.040	2.166	0.468	0.548	0.819	1.070
	BRGB	1.515	3.710	0.831	2.917	0.892	0.918	1.495	2.000
	TRGB	1.547	3.516	3.353	-0.534	1.608	3.060	4.834	6.097
9.3	TO	1.471	3.666	1.779	0.766	1.121	1.115	1.863	2.518
	BRGB	1.471	3.621	1.779	0.766	1.121	1.115	1.863	2.518
	TRGB	1.471	3.621	1.779	0.766	1.121	1.115	1.863	2.518
	TO	1.423	3.818	0.737	2.926	0.454	0.533	0.792	1.034
	B	1.604	3.791	0.998	2.296	0.549	0.622	0.945	1.241
9.2	TO	1.615	3.824	1.169	1.835	0.422	0.502	0.743	0.968
	C	1.627	3.711	0.933	2.654	0.887	0.913	1.486	1.984
	BRGB	1.627	3.711	0.933	2.654	0.887	0.913	1.486	1.984
	TRGB	1.627	3.711	0.933	2.654	0.887	0.913	1.486	1.984
	TO	1.635	3.424	3.951	0.128	1.626	4.541	7.268	8.635
9.1	TO	1.635	3.424	3.951	0.128	1.626	4.541	7.268	8.635
	C	1.729	3.800	1.134	1.946	0.516	0.591	0.893	1.169
	BRGB	1.729	3.800	1.134	1.946	0.516	0.591	0.893	1.169
	TRGB	1.729	3.800	1.134	1.946	0.516	0.591	0.893	1.169
	TO	1.742	3.842	1.303	1.483	0.363	0.435	0.635	0.824
9.0	TO	1.754	3.712	1.044	2.375	0.887	0.912	1.482	1.980
	C	1.754	3.712	1.044	2.375	0.887	0.912	1.482	1.980
	BRGB	1.754	3.712	1.044	2.375	0.887	0.912	1.482	1.980
	TRGB	1.754	3.712	1.044	2.375	0.887	0.912	1.482	1.980
	TO	1.814	3.424	3.998	0.010	1.626	4.539	7.265	8.632
8.9	TO	1.814	3.424	3.998	0.010	1.626	4.539	7.265	8.632
	C	1.873	3.811	1.284	1.555	0.469	0.548	0.822	1.075
	BRGB	1.873	3.811	1.284	1.555	0.469	0.548	0.822	1.075
	TRGB	1.873	3.811	1.284	1.555	0.469	0.548	0.822	1.075
	TO	1.885	3.865	1.445	1.103	0.275	0.316	0.483	0.621
8.8	TO	1.885	3.865	1.445	1.103	0.275	0.316	0.483	0.621
	C	1.896	3.711	1.166	2.072	0.893	0.914	1.486	1.986
	BRGB	1.896	3.711	1.166	2.072	0.893	0.914	1.486	1.986
	TRGB	1.896	3.711	1.166	2.072	0.893	0.914	1.486	1.986
	TO	1.924	3.778	2.968	-1.433	1.552	1.755	2.829	3.870
8.7	TO	1.924	3.778	2.968	-1.433	1.552	1.755	2.829	3.870
	C	1.949	3.679	1.763	0.723	1.055	1.050	1.742	2.347
	BRGB	1.949	3.679	1.763	0.723	1.055	1.050	1.742	2.347
	TRGB	1.949	3.679	1.763	0.723	1.055	1.050	1.742	2.347
	TO	2.022	3.827	1.423	1.195	0.408	0.488	0.722	0.938
8.6	TO	2.022	3.827	1.423	1.195	0.408	0.488	0.722	0.938
	C	2.037	3.889	1.581	0.761	0.187	0.210	0.330	0.427
	BRGB	2.037	3.889	1.581	0.761	0.187	0.210	0.330	0.427
	TRGB	2.037	3.889	1.581	0.761	0.187	0.210	0.330	0.427
	TO	2.071	3.713	1.283	-0.966	1.427	1.988	4.172	1.966
8.5	TO	2.071	3.713	1.283	-0.966	1.427	1.988	4.172	1.966
	C	2.290	3.446	1.165	-0.926	1.622	4.180	6.680	8.024
	BRGB	2.290	3.446	1.165	-0.926	1.622	4.180	6.680	8.024
	TRGB	2.290	3.446	1.165	-0.926	1.622	4.180	6.680	8.024
	TO	2.190	3.849	1.571	0.799	0.352	0.395	0.582	0.753
8.4	TO	2.190	3.849	1.571	0.799	0.352	0.395	0.582	0.753
	C	2.207	3.913	1.727	0.412	0.111	0.125	0.202	0.257
	BRGB	2.207	3.913	1.727	0.412	0.111	0.125	0.202	0.257
	TRGB	2.207	3.913	1.727	0.412	0.111	0.125	0.202	0.257
	TO	2.218	3.712	1.417	1.438	0.892	0.909	1.474	1.972
8.3	TO	2.218	3.712	1.417	1.438	0.892	0.909	1.474	1.972
	C	2.333	3.634	2.425	-0.624	1.295	1.288	2.168	2.946
	BRGB	2.333	3.634	2.425	-0.624	1.295	1.288	2.168	2.946
	TRGB	2.333	3.634	2.425	-0.624	1.295	1.288	2.168	2.946
	TO	2.493	3.448	4.221	-1.090	1.622	4.163	6.652	7.996
8.2	TO	2.493	3.448	4.221	-1.090	1.622	4.163	6.652	7.996
	C	2.500	3.918	1.730	1.261	0.124	0.124	0.191	0.248
	BRGB	2.500	3.918	1.730	1.261	0.124	0.124	0.191	0.248
	TRGB	2.500	3.918	1.730	1.261	0.124	0.124	0.191	0.248
	TO	2.411	3.940	1.881	0.085	0.046	0.051	0.091	0.113
8.1	TO	2.411	3.940	1.881	0.085	0.046	0.051	0.091	0.113
	C	2.421	3.710	1.562	1.084	0.906	0.918	1.490	1.994
	BRGB	2.421	3.710	1.562	1.084	0.906	0.918	1.490	1.994
	TRGB	2.421	3.710	1.562	1.084	0.906	0.918	1.490	1.994
	TO	2.574	3.693	1.872	0.379	0.991	0.986	1.627	2.178
8.0	TO	2.574	3.693	1.872	0.379	0.991	0.986	1.627	2.178
	C	2.713	3.448	4.278	-1.243	1.621	4.156	6.640	7.983
	BRGB	2.713	3.448	4.278	-1.243	1.621	4.156	6.640	7.983
	TRGB	2.713	3.448	4.278	-1.243	1.621	4.156	6.640	7.983
	TO	2.615	3.904	1.892	-0.210	-0.011	0.001	-0.002	-0.003
7.9	TO	2.615	3.904	1.892	-0.210	-0.011	0.001	-0.002	-0.003
	C	2.636	3.968	2.039	-0.017	0.130	0.149	0.246	0.315
	BRGB	2.636	3.968	2.039	-0.017	0.130	0.149	0.246	0.315
	TRGB	2.636	3.968	2.039	-0.017	0.130	0.149	0.246	0.315
	TO	2.646	3.707	1.712	0.921	0.921	0.928	1.511	2.020
7.8	TO	2.646	3.707	1.712	0.921	0.921	0.928	1.511	2.020
	C	2.857	3.634	2.584	-1.021	1.302	1.287	2.168	2.945
	BRGB	2.857	3.634	2.584	-1.021	1.302	1.287	2.168	2.945
	TRGB	2.857	3.634	2.584	-1.021	1.302	1.287	2.168	2.945
	TO	2.794	3.694	1.973	0.124	0.991	0.984	1.623	2.172
7.7	TO	2.794	3.694	1.973	0.124	0.991	0.984	1.623	2.172
	C	2.850	3.971	1.755	0.511	0.002	0.001	-0.008	-0.008
	BRGB	2.850	3.971	1.755	0.511	0.002	0.001	-0.008	-0.008
	TRGB	2.850	3.971	1.755	0.511	0.002	0.001	-0.008	-0.008
	TO	2.850	3.971	1.755	0.511	0.002	0.001	-0.008	-0.008
7.6	TO	2.850	3.971	1.755	0.511	0.002	0.001	-0.008	-0.008
	C	2.878	3.995	2.195	-0.488	-0.049	-0.035	-0.070	-0.086
	BRGB	2.878	3.995	2.195	-0.488	-0.049	-0.035	-0.070	-0.086
	TRGB	2.878	3.995	2.195	-0.488	-0.049	-0.035	-0.070	-0.086
	TO	2.886	3.705	1.866	0.343	0.938	0.939	1.535	2.051
7.5	TO	2.886	3.705	1.866	0.343	0.938	0.939	1.535	2.051
	C	2.895	3.633	2.671	-1.232	1.310	1.291	2.176	2.956
	BRGB	2.895	3.633	2.671	-1.232	1.310	1.291	2.176	2.956
	TRGB	2.895	3.633	2.671	-1.232	1.310	1.291	2.176	2.956
	TO	3.046	3.694	2.108	-0.046	0.994	0.985	1.625	2.176
7.4	TO	3.046	3.694	2.108	-0.046	0.994	0.985	1.625	2.176
	C	3.199	3.449	4.389	-1.546	4.137	6.610	7.952	9.521
	BRGB	3.199	3.449	4.389	-1.546	4.137	6.610	7.952	9.521
	TRGB	3.199	3.449	4.389	-1.546	4.137	6.610	7.952	9.521
	TO	2.750	3.998	1.913	0.229	-0.041	-0.038	-0.076	-0.095
7.3	TO	2.750	3.998	1.913	0.229	-0.041	-0.038	-0.076	-0.095
	C	3.133	3.961	2.221	-0.693	-0.011	0.009	0.018	0.022
	BRGB	3.133	3.961	2.221	-0.693	-0.011	0.009	0.018	0.022
	TRGB	3.133	3.961	2.221	-0.693	-0.011	0.009	0.018	0.022
	TO	3.133	3.961	2.221	-0.693	-0.011	0.009	0.018	0.022

Table 10. continued

 $Z = 0.008 \quad Y = 0.250$ 

Age	Phase	M	$T_{\text{eff}}$	L	$M_V$	B-V	V-I	V-J	V-K
6.9	$M_{\text{Heb}}$	19.760	4.114	5.142	-7.216	-0.130	-0.080	-0.250	-0.320
	LM	20.232	3.596	5.331	-7.511	1.536	1.586	2.634	3.583
	TO	17.200	4.484	4.667	-3.964	-0.284	-0.302	-0.690	-0.916
	B	23.844	4.368	5.181	-5.898	-0.234	-0.234	-0.567	-0.750
	C	24.031	4.423	5.239	-5.733	-0.254	-0.269	-0.627	-0.832
6.8	$R_{\text{Heb}}$	24.031	4.423	5.239	-5.733	-0.254	-0.269	-0.627	-0.832
	$B_{\text{Heb}}$	24.557	4.129	5.204	-7.528	-0.125	-0.080	-0.259	-0.338
	$M_{\text{Heb}}$	24.962	4.002	5.315	-8.220	-0.061	0.009	-0.053	-0.074
	LM	25.773	3.669	5.486	-8.512	1.249	1.148	1.877	2.478
	TO	20.000	4.509	4.853	-4.302	-0.290	-0.310	-0.710	-0.943
6.7	B	29.297	4.363	5.332	-6.430	-0.231	-0.231	-0.561	-0.742
	C	29.481	4.418	5.482	-6.264	-0.247	-0.259	-0.617	-0.819
	$R_{\text{Heb}}$	29.630	3.701	5.484	-8.700	1.023	0.983	1.570	2.060
	$M_{\text{Heb}}$	30.154	4.101	5.490	-8.155	-0.122	-0.072	-0.227	-0.297
	LM	31.104	3.788	5.480	-8.976	0.441	0.588	0.871	1.141
6.6	$M_{\text{Heb}}$	32.406	4.100	5.646	-8.552	-0.122	-0.072	-0.225	-0.295
	LM	24.400	4.535	5.021	-4.580	-0.293	-0.310	-0.710	-0.950
	TO	24.400	4.535	5.021	-4.580	-0.293	-0.310	-0.710	-0.950
	B	38.670	4.318	5.607	-7.226	-0.218	-0.218	-0.517	-0.685
	C	38.670	4.364	5.646	-7.081	-0.231	-0.231	-0.563	-0.744
6.6	B	38.910	4.364	5.646	-7.081	-0.231	-0.231	-0.563	-0.744
	C	38.910	4.364	5.646	-7.081	-0.231	-0.231	-0.563	-0.744
	LM	45.062	5.251	5.804	-1.609	-0.880	-0.400	-0.880	-1.170
	TO	29.300	4.561	5.217	-4.909	-0.306	-0.316	-0.721	-0.961
	B	53.178	4.267	5.804	-8.016	-0.185	-0.175	-0.450	-0.590
6.6	B	53.178	4.267	5.804	-8.016	-0.185	-0.175	-0.450	-0.590
	C	56.874	4.468	5.900	-7.160	-0.274	-0.290	-0.670	-0.894
	LM	71.644	5.292	5.534	-0.656	-0.388	-0.403	-0.885	-1.177
	C	71.644	5.292	5.534	-0.656	-0.388	-0.403	-0.885	-1.177
	LM	71.644	5.292	5.534	-0.656	-0.388	-0.403	-0.885	-1.177

Table 11. continued

Z = 0.02    Y = 0.280													
Age	Phase	M	T <sub>eff</sub>	L	M <sub>V</sub>	B-V	V-I	V-J	V-K				
8.4	C	3.160	4.023	2.357	-0.761	-0.077	-0.054	-0.124	-0.165				
	B <sub>RGB</sub>	3.170	3.701	2.030	-0.954	0.955	0.951	1.560	2.084				
	T <sub>RGB</sub>	3.339	3.630	2.789	-1.497	1.333	1.311	2.212	3.006				
	M <sub>Heb</sub>	3.379	3.692	2.263	-0.594	1.007	0.993	1.639	2.194				
	T <sub>AGB</sub>	3.482	3.450	4.442	-1.696	1.621	4.126	6.591	7.932				
	TO	3.500	4.026	2.104	-0.116	-0.070	-0.060	-0.130	-0.172				
	B	3.458	3.989	2.391	-0.996	-0.051	-0.030	-0.061	-0.071				
	C	3.484	4.052	2.523	-1.033	-0.101	-0.077	-0.176	-0.232				
	B <sub>RGB</sub>	3.493	3.698	2.202	-0.473	0.912	0.963	1.585	2.117				
	T <sub>RGB</sub>	3.501	3.624	2.930	-1.797	1.370	1.347	2.276	3.097				
8.3	M <sub>Heb</sub>	3.642	3.690	2.428	-0.998	1.022	1.001	1.654	2.215				
	T <sub>AGB</sub>	3.764	3.452	4.488	-1.863	1.621	4.090	6.533	7.872				
	TO	3.400	4.055	2.280	-0.410	-0.093	-0.082	-0.181	-0.237				
	B	3.783	4.018	2.562	-1.297	-0.078	-0.049	-0.115	-0.152				
	C	3.809	4.081	2.689	-1.294	-0.118	-0.093	-0.222	-0.293				
	B <sub>RGB</sub>	3.816	3.695	2.375	-0.890	0.993	0.977	1.611	2.153				
	T <sub>RGB</sub>	3.822	3.620	3.059	-2.073	1.404	1.379	2.335	3.180				
	M <sub>Heb</sub>	3.934	3.688	2.581	-1.371	1.036	1.009	1.668	2.234				
	T <sub>AGB</sub>	4.067	3.454	4.539	-2.030	1.620	4.063	6.489	7.826				
	TO	3.700	4.083	2.423	-0.614	-0.115	-0.100	-0.227	-0.297				
8.2	C	4.149	4.047	2.736	-1.589	-0.103	-0.072	-0.168	-0.221				
	B <sub>RGB</sub>	4.183	4.109	2.859	-1.565	-0.126	-0.108	-0.262	-0.343				
	T <sub>RGB</sub>	4.192	3.690	2.553	-1.312	1.024	1.001	1.653	2.212				
	M <sub>Heb</sub>	4.198	3.613	3.218	-2.400	1.448	1.428	2.418	3.300				
	T <sub>AGB</sub>	4.337	3.686	2.790	-1.884	1.056	1.019	1.686	2.298				
	TO	4.472	4.384	2.270	-1.619	1.619	3.975	6.343	7.676				
	C	4.595	4.076	2.916	-1.888	-0.118	-0.087	-0.213	-0.281				
	B <sub>RGB</sub>	4.628	4.138	3.035	-1.843	-0.144	-0.125	-0.300	-0.395				
	T <sub>RGB</sub>	4.635	3.682	2.740	-1.740	1.071	1.035	1.716	2.304				
	M <sub>Heb</sub>	4.641	3.606	3.388	-2.749	1.491	1.483	2.507	3.428				
8.1	T <sub>AGB</sub>	4.748	3.583	2.993	-2.385	1.071	1.025	1.697	2.268				
	TO	4.877	3.462	4.647	-2.481	1.619	3.937	6.284	7.613				
	C	5.050	4.142	2.760	-1.135	-0.140	-0.127	-0.304	-0.403				
	B	5.050	4.104	3.094	-2.181	-0.126	-0.103	-0.252	-0.332				
	C	5.091	4.166	3.211	-2.121	-0.156	-0.137	-0.337	-0.444				
	B <sub>RGB</sub>	5.099	3.675	2.927	-2.167	1.116	1.068	1.779	2.390				
	T <sub>RGB</sub>	5.105	3.599	3.555	-3.093	1.518	1.545	2.592	3.544				
	M <sub>Heb</sub>	5.223	3.687	3.211	-2.941	1.072	1.018	1.682	2.240				
	T <sub>AGB</sub>	5.370	3.474	4.658	-2.773	1.617	3.753	5.984	7.302				
	TO	4.950	4.171	2.929	-1.388	-0.152	-0.144	-0.343	-0.451				
7.9	C	5.617	4.132	3.275	-2.476	-0.142	-0.119	-0.292	-0.383				
	B <sub>RGB</sub>	5.655	4.194	3.388	-2.400	-0.173	-0.153	-0.376	-0.493				
	T <sub>RGB</sub>	5.661	3.670	3.115	-2.605	1.150	1.093	1.830	2.456				
	M <sub>Heb</sub>	5.780	3.692	3.437	-3.535	1.055	0.998	1.639	2.173				
	T <sub>AGB</sub>	5.865	3.595	3.728	-3.485	1.529	1.587	2.643	3.610				
	TO	5.900	3.487	4.658	-3.082	1.614	3.540	5.636	6.940				
	C	5.500	4.200	3.098	-1.640	-0.170	-0.158	-0.384	-0.502				
	B	6.224	4.160	3.455	-2.771	-0.155	-0.133	-0.328	-0.431				
	C	6.270	4.222	3.566	-2.682	-0.187	-0.167	-0.411	-0.538				
	T <sub>RGB</sub>	6.277	3.662	3.298	-3.020	1.195	1.127	1.898	2.549				
7.7	T <sub>AGB</sub>	6.282	3.583	3.893	-3.790	1.704	2.776	3.791	4.791				
	B <sub>Heb</sub>	6.356	3.634	3.502	-3.313	1.356	1.286	2.183	2.956				
	M <sub>Heb</sub>	6.388	3.753	3.651	-4.296	0.723	0.748	1.169	1.536				
	C	6.408	3.719	3.648	-4.186	0.908	0.885	1.416	1.868				
	LM	6.515	3.535	4.345	-3.770	1.596	2.614	4.006	5.186				
	TO	6.100	4.229	3.274	-1.908	-0.183	-0.175	-0.418	-0.548				
	B	6.925	4.187	3.638	-3.070	-0.168	-0.146	-0.364	-0.478				
	C	6.968	4.250	3.745	-2.966	-0.198	-0.185	-0.444	-0.581				
	B <sub>RGB</sub>	6.974	3.652	3.474	-3.392	1.259	1.180	1.998	2.690				
	T <sub>RGB</sub>	6.979	3.574	4.064	-4.124	1.560	1.805	2.887	3.947				
6.9	R <sub>Heb</sub>	7.069	3.623	3.706	-3.725	1.426	1.354	2.304	3.129				
	B <sub>Heb</sub>	7.113	3.791	3.858	-4.912	0.507	0.568	0.893	1.165				
	M <sub>Heb</sub>	7.138	3.750	3.858	-4.807	0.743	0.762	1.192	1.565				
	LM	7.251	3.544	4.338	-4.123	1.590	2.393	3.602	4.741				
	B	7.251	3.544	4.338	-4.123	1.590	2.393	3.602	4.741				
	LM	7.251	3.544	4.338	-4.123	1.590	2.393	3.602	4.741				
	LM	7.251	3.544	4.338	-4.123	1.590	2.393	3.602	4.741				
	LM	7.251	3.544	4.338	-4.123	1.590	2.393	3.602	4.741				
	LM	7.251	3.544	4.338	-4.123	1.590	2.393	3.602	4.741				
	LM	7.251	3.544	4.338	-4.123	1.590	2.393	3.602	4.741				

Table 11. continued

 $Z = 0.02 \quad Y = 0.280$ 

Age	Phase	M	$T_{eff}$	L	M <sub>V</sub>	B-V	V-I	V-J	V-K
6.8	C	21.790	4.372	5.175	-5.908	-0.236	-0.576	-0.767	
	BRGB	21.825	3.610	5.045	-6.916	1.511	1.471	2.502	3.356
	TRGB	21.835	3.582	5.243	-7.151	1.551	1.721	2.799	3.809
	RHeb	22.081	3.623	5.165	-7.351	1.481	1.383	2.356	3.137
	MHeb	22.765	3.754	5.186	-8.160	0.717	0.729	1.142	1.489
	BHeb	23.515	3.785	5.259	-8.426	0.521	0.564	0.903	1.171
	LM	34.591	3.765	5.406	-8.750	0.643	0.663	1.051	1.366
	TO	18.400	4.476	4.765	-4.290	-0.275	-0.296	-0.685	-0.915
	B	27.200	4.265	5.314	-6.842	-0.187	-0.176	-0.454	-0.603
	C	27.416	4.326	5.368	-6.629	-0.220	-0.222	-0.534	-0.706
6.7	LM	29.344	4.111	5.554	-8.291	-0.128	-0.088	-0.246	-0.333
	TO	21.200	4.502	4.906	-4.502	-0.287	-0.309	-0.707	-0.946
	B	34.874	4.111	5.507	-8.172	-0.128	-0.088	-0.247	-0.334
	C	35.728	4.282	5.577	-7.413	-0.193	-0.184	-0.475	-0.627
	LM	42.430	5.197	5.120	-10.284	-0.378	-0.406	-0.884	-1.178
6.6	TO	26.000	4.527	5.094	-4.830	-0.290	-0.310	-0.720	-0.960
	B	45.338	4.077	5.677	-8.786	-0.119	-0.059	-0.197	-0.265
	C	51.800	4.476	5.841	-7.008	-0.270	-0.290	-0.679	-0.909
	LM	67.942	5.252	5.146	0.025	-0.380	-0.410	-0.890	-1.185

Table 12.

 $Z = 0.05 \quad Y = 0.352$ 

Age	Phase	M	$T_{eff}$	L	M <sub>V</sub>	B-V	V-I	V-J	V-K
10.2	TO	0.876	3.723	-0.035	5.033	0.832	0.890	1.419	1.869
	BRGB	0.905	3.689	0.153	4.723	1.031	1.041	1.697	2.262
	TRGB	0.919	3.609	3.387	1.954	1.679	4.827	1.679	9.120
	MHeb	0.711	3.634	1.706	1.196	1.375	1.314	2.223	2.977
	TAGB	0.712	3.440	3.352	1.257	1.673	4.285	1.651	8.202
10.1	TO	0.919	3.731	0.027	4.853	0.850	0.863	1.355	1.778
	BRGB	0.955	3.692	0.213	4.558	1.022	1.028	1.676	2.231
	TRGB	0.970	3.412	3.393	1.794	1.678	4.726	1.751	8.949
	MHeb	0.778	3.629	1.723	1.195	1.399	1.344	2.277	3.053
	TAGB	0.780	3.394	3.549	1.794	1.681	4.991	8.002	9.397
10.0	TO	0.955	3.694	0.058	4.751	0.817	0.837	1.288	1.685
	BRGB	1.005	3.694	0.274	4.390	1.011	1.012	1.651	2.195
	TRGB	1.026	3.420	3.391	1.617	1.677	4.602	7.368	8.739
	MHeb	0.852	3.629	1.746	1.142	1.401	1.349	2.288	3.064
	TAGB	0.855	3.372	3.662	1.927	1.684	5.256	8.435	9.847
9.9	TO	1.002	3.748	0.152	4.486	0.780	0.796	1.233	1.607
	BRGB	1.065	3.692	0.337	4.246	1.024	1.025	1.625	2.229
	TRGB	1.088	3.428	3.390	1.432	1.675	4.471	7.153	8.516
	MHeb	0.934	3.628	1.758	1.117	1.400	1.351	2.288	3.070
	TAGB	0.938	3.365	3.737	1.887	1.685	5.351	8.591	10.008
9.8	TO	1.065	3.758	0.269	4.160	0.741	0.754	1.176	1.526
	BRGB	1.130	3.691	0.402	4.089	1.028	1.028	1.681	2.238
	TRGB	1.160	3.435	3.388	1.284	1.674	4.365	6.982	8.338
	MHeb	1.022	3.629	1.768	1.081	1.392	1.345	2.275	3.052
	TAGB	1.028	3.363	3.804	1.765	1.685	5.381	8.639	10.058
9.7	TO	1.137	3.767	0.397	3.815	0.702	0.714	1.108	1.438
	BRGB	1.202	3.692	0.466	3.922	1.025	1.022	1.673	2.226
	TRGB	1.236	3.442	3.388	1.111	1.672	4.245	6.785	8.133
	MHeb	1.112	3.631	1.779	1.043	1.383	1.336	2.259	3.031
	TAGB	1.119	3.361	3.864	1.637	1.685	5.395	8.661	10.081
9.6	TO	1.220	3.777	0.535	3.444	0.663	0.673	1.035	1.346
	BRGB	1.277	3.692	0.527	3.766	1.024	1.019	1.689	2.219
	TRGB	1.319	3.452	3.385	0.903	1.671	4.097	6.641	7.883
	MHeb	1.210	3.633	1.787	1.002	1.368	1.321	2.231	2.992
	TAGB	1.223	3.359	3.933	1.518	1.685	5.430	8.719	10.140
9.5	TO	1.325	3.787	0.704	3.010	0.619	0.639	0.974	1.258
	BRGB	1.389	3.695	0.657	3.427	1.016	1.005	1.648	2.188
	TRGB	1.420	3.463	3.361	0.707	1.689	3.919	6.254	7.582
	MHeb	1.331	3.637	1.794	0.957	1.348	1.301	2.254	2.941
	TAGB	1.347	3.359	3.998	1.358	1.685	5.430	8.720	10.141
9.4	TO	1.332	3.777	0.544	3.424	0.664	0.676	1.038	1.349
	BRGB	1.462	3.768	0.753	2.921	0.701	0.710	1.102	1.429
	B	1.476	3.796	0.943	2.399	0.581	0.606	0.917	1.177
	C	1.491	3.695	0.760	3.167	1.017	1.003	1.646	2.185
	BRGB	1.491	3.695	0.760	3.167	1.017	1.003	1.646	2.185

Table 12. continued

 $Z = 0.05 \quad Y = 0.352$ 

Age	Phase	M	$T_{\text{eff}}$	L	$M_V$	B-V	V-I	V-J	V-K
8.4	TAGB	3.255	3.395	4.362	-0.260	1.681	4.978	7.981	9.375
	TO	2.800	3.986	1.923	0.118	-0.031	-0.027	-0.061	-0.079
	B	3.200	3.965	2.245	-0.768	-0.016	0.001	-0.006	-0.014
	C	3.245	4.032	2.417	-0.896	-0.097	-0.158	-0.158	-0.208
8.3	BRGB	3.264	3.678	2.061	-0.007	1.142	1.075	1.789	2.366
	TRGB	3.256	3.999	2.847	-0.299	1.299	1.562	2.649	3.577
	MHeb	3.389	3.655	2.351	-0.580	1.269	1.193	2.001	2.669
	TAGB	3.326	3.395	4.417	-0.398	1.681	4.976	7.978	9.372
8.2	TO	3.100	4.013	2.117	-0.239	-0.068	-0.125	-0.159	-0.159
	B	3.500	3.992	2.409	-1.066	-0.057	-0.036	-0.079	-0.102
	C	3.547	4.061	2.581	-1.164	-0.116	-0.090	-0.209	-0.279
	BRGB	3.556	3.673	2.225	-0.388	1.172	1.099	1.833	2.427
8.1	TRGB	3.563	3.592	2.994	-1.614	1.545	1.622	2.705	3.667
	MHeb	3.681	3.650	2.507	-0.934	1.302	1.219	2.053	2.738
	TAGB	3.798	3.496	4.465	-0.552	1.680	4.955	7.944	9.337
	TO	3.400	4.042	2.273	-0.489	-0.098	-0.080	-0.177	-0.231
8.0	B	3.819	4.020	2.594	-1.396	-0.134	-0.106	-0.138	-0.179
	C	3.849	4.089	2.745	-1.431	-0.134	-0.106	-0.247	-0.333
	BRGB	3.857	3.669	2.389	-0.767	1.203	1.124	1.877	2.489
	TRGB	3.862	3.587	3.130	-1.910	1.555	1.670	2.753	3.740
7.9	MHeb	3.973	3.645	2.663	-1.283	1.337	1.249	2.111	2.815
	TAGB	4.096	3.400	4.509	-0.729	1.680	4.912	7.874	9.264
	TO	3.750	4.070	2.463	-0.825	-0.117	-0.095	-0.222	-0.297
	B	4.165	4.048	2.763	-1.681	-0.114	-0.081	-0.184	-0.247
8.0	C	4.203	4.117	2.911	-1.690	-0.150	-0.113	-0.286	-0.385
	BRGB	4.213	3.664	2.558	-1.156	1.235	1.148	1.922	2.551
	TRGB	4.219	3.579	3.284	-2.228	1.571	1.747	2.829	3.856
	MHeb	4.338	3.636	2.825	-1.616	1.390	1.299	2.205	2.946
7.8	TAGB	4.476	3.401	4.569	-0.914	1.680	4.889	7.835	9.224
	TO	4.050	4.098	2.611	-1.046	-0.135	-0.110	-0.262	-0.352
	B	4.574	4.076	2.934	-1.972	-0.128	-0.096	-0.226	-0.304
	C	4.612	4.145	3.079	-1.953	-0.159	-0.130	-0.328	-0.429
7.7	BRGB	4.620	3.659	2.731	-1.536	1.268	1.172	1.970	2.616
	TRGB	4.625	3.570	3.447	-2.492	1.591	1.882	2.980	4.051
	MHeb	4.737	3.627	3.011	-1.994	1.450	1.359	2.315	3.102
	TAGB	4.855	3.405	4.621	-1.126	1.679	4.831	7.741	9.126
7.6	TO	4.500	4.126	2.795	-1.350	-0.149	-0.123	-0.302	-0.401
	B	4.983	4.103	3.105	-2.258	-0.144	-0.109	-0.286	-0.359
	C	5.026	4.173	3.248	-2.217	-0.169	-0.146	-0.366	-0.475
	BRGB	5.034	3.653	2.905	-1.955	1.304	1.198	2.024	2.688
7.5	TRGB	5.040	3.561	3.604	-2.678	1.610	2.059	3.195	4.290
	MHeb	5.163	3.617	3.189	-2.341	1.492	1.426	2.433	3.267
	TAGB	5.315	3.417	4.650	-1.473	1.677	4.642	7.433	8.807
	TO	4.900	4.154	2.952	-1.583	-0.159	-0.139	-0.341	-0.449
7.4	B	5.510	4.130	3.280	-2.542	-0.155	-0.120	-0.304	-0.404
	C	5.556	4.201	3.420	-2.489	-0.179	-0.168	-0.396	-0.524
	BRGB	5.563	3.647	3.078	-2.337	1.347	1.235	2.097	2.787
	TRGB	5.569	3.554	3.763	-2.904	1.625	2.206	3.374	4.488
7.3	MHeb	5.692	3.605	3.391	-2.721	1.530	2.580	3.471	3.471
	TAGB	5.824	3.434	4.666	-1.904	1.674	4.371	6.990	8.347
	TO	5.400	4.183	3.117	-1.833	-0.172	-0.155	-0.377	-0.496
	B	6.050	4.157	3.455	-2.837	-0.165	-0.136	-0.343	-0.449
7.2	C	6.109	4.228	3.593	-2.763	-0.199	-0.179	-0.437	-0.567
	BRGB	6.122	3.546	3.920	-3.116	1.637	2.361	3.563	4.697
	TRGB	6.263	3.594	3.584	-3.098	1.553	1.610	2.698	3.644
	MHeb	6.376	3.493	4.360	-2.476	1.663	3.430	5.478	6.776
7.1	TO	5.950	4.211	3.293	-2.106	-0.184	-0.173	-0.411	-0.541
	B	6.717	4.183	3.635	-3.131	-0.176	-0.151	-0.378	-0.493
	C	6.773	4.255	3.769	-3.056	-0.209	-0.199	-0.470	-0.620
	BRGB	6.785	3.626	3.425	-3.029	1.475	1.362	2.325	3.106
7.0	TRGB	6.912	3.562	4.084	-3.124	1.646	2.610	4.000	5.179
	MHeb	7.023	3.508	4.302	-2.662	1.661	3.214	5.104	6.388
	TO	6.550	4.240	3.443	-2.319	-0.200	-0.188	-0.452	-0.588